Macrobrachium rosenbergii nodavirus virus-like particles attach to fucosylated glycans in the gills of the giant freshwater prawn

Monsicha Somrit, Shin-Yi Yu, Jacques Le Pendu, Adrien Breiman, Yann Guerardel, Wattana Weerachatyanukul, Atthaboon Watthammawut

Macrobrachium rosenbergii nodavirus virus-like particles attach to fucosylated glycans in the gills of the giant freshwater prawn

Monsicha Somrit[1], Shin-Yi Yu[2], Jacques Le Pendu[3], Adrien Breiman[3,4], Yann Guerardel[2], Wattana Weerachatyanukul[1], Atthaboon Watthammawut[5*]

[1]Department of Anatomy, Faculty of Science, Mahidol University, Rama VI Road, Bangkok, Thailand, 10400

[2]Université de Lille, CNRS, UMR 8576-UGSF-Unité de Glycobiologie Structurale et Fonctionnelle, F-59000 Lille, France

[3]Université de Nantes, Inserm, CRCINA, F-44000, Nantes, France

[4]Centre Hospitalier Universitaire de Nantes, Nantes, France

[5]Department of Anatomy, Faculty of Medicine, Srinakharinwirot University, Bangkok, Thailand, 10110

*Correspondence should be addressed to:

Dr. Atthaboon Watthammawut

Department of Anatomy, Faculty of Medicine, Srinakharinwirot University,

Bangkok, Thailand, 10110

Tel.: +66(0)617300110

E-mail: atthaboon@g.swu.ac.th

ABSTRACT

The Macrobrachium rosenbergii nodavirus (MrNV), the causative agent of white-tail disease (WTD) in many species of shrimp and prawn, has been shown to infect hemocytes and tissues such as the gills and muscles. However, little is known about the host surface molecules to which MrNV attach to initiate infection. Therefore, the present study investigated the role of glycans as binding molecules for virus attachment in susceptible tissues such as the gills. We established that MrNV in their virus-like particle (MrNV-VLP) form exhibited strong binding to gill tissues and lysates, which was highly reduced by the glycan-reducing periodate and PNGase F. The broad fucose-binding *Aleuria Aurantia* lectin (AAL) was highly reduced MrNV-VLPs binding to gill tissue sections and lysates, and efficiently disrupted the specific interactions between the VLPs and gill glycoproteins. Furthermore, mass spectroscopy revealed the existence of unique fucosylated LacdiNAc-extended *N*-linked and *O*-linked glycans in the gill tissues, whereas beta-elimination experiments showed that MrNV-VLPs demonstrated a binding preference for *N*-glycans. Therefore, the results from this study highly suggested that MrNV-VLPs preferentially attach to fucosylated *N*-glycans in the susceptible gill tissues, and these findings could lead to the development of strategies that target virus-host surface glycan interactions to reduce MrNV infections.

INTRODUCTION

Macrobrachium rosenbergii nodavirus (MrNV) is the primary causative agent of the white tail disease (WTD) in the giant freshwater prawn *Macrobrachium rosenbergii* (de Man, 1879). Characterized by the distinctive whitish discoloration in the muscle tissues of post-larvae prawn, WTD ultimately results as a 100% rate of sudden mortality among post-larvae and in extensive damage to giant freshwater prawn aquaculture (Azad et al., 2005; J. R. Bonami, Z. Shi, D. Qian, & J. Sri Widada, 2005). MrNV, along with its closely related Penaeus vannamei nodavirus (PvNV), has been shown to infect a broad spectrum of cells and organisms, ranging from mosquito cell cultures (C6/36) and aquatic insects to other types of prawn such as *Penaeus monodon* and *Penaeus vannamei* (Hayakijkosol & Owens, 2013; Sahul Hameed, Yoganandhan, Sri Widada, & Bonami, 2004; Sudhakaran et al., 2008; Sudhakaran, Parameswaran, & Sahul Hameed, 2007). MrNV is a single-protein capsid non-enveloped virus, with a single-stranded RNA+ bipartite genome, and exhibits a T=3 icosahedral conformation. Phylogenetic and structural analyses based on the amino acid sequences of the RNA2 region encoding the capsid protein suggests that MrNV could be classified in its own genus *Gammanodavirus,* distinct from the insect and fish infecting *Alpha*- and *Betanodavirus* genera (Ho et al., 2018; NaveenKumar, Shekar, Karunasagar, & Karunasagar, 2013). MrNV virus-like particles (MrNV-VLPs) can be generated from the expression in either bacterial or insect-based systems of the capsid gene of RNA2, and they appear structurally identical to infectious MrNV virions (J.-R. Bonami, Z. Shi, D. Qian, & J. Sri Widada, 2005; Bonami & Widada, 2011; Ho, Kueh, Beh, Tan, & Bhella, 2017).

The molecular structure of the MrNV capsid has been extensively described, comprising primarily an internal capsid shell (S-domains of the capsid protein subunits) and the external protruding spikes (subunit P-domains) (Ho et al., 2017). We previously reported the successful infection and propagation of MrNV in the Sf9 insect cell line and its dependence

on caveolin-dependent endocytosis for internalization into susceptible cells (M. Somrit, Watthammawut, Chotwiwatthanakun, & Weerachatyanukul, 2016). Furthermore, we demonstrated that the amino acids T345-N371 at the C-terminus was crucial for binding and internalization of the virus into Sf9 cells (Monsicha Somrit et al., 2017). Nevertheless, the specific surface binding factors that the virus uses to enter Sf9 cells or susceptible prawn tissues have yet to be fully elucidated.

Given the fact that MrNV has the ability to infect a broad spectrum of hosts as described above, can infect most tissues and hemocytes in *M. rosenbergii* yet specifically causes pathogenesis (WTD) in the muscle tissues (Hameed, Yoganandhan, Widada, & Bonami, 2004; Jean-Michel et al., 1999; Sri Widada et al., 2003), led us to suspect that the virus may not depend on only proteinaceous host surface receptors but maybe also on glycosylated host surface molecules as binding factors. These broad yet selective characteristics are similar to the noroviruses of the *Caliciviridae*, which interact with *N-/O*-linked fucosylated glycans of human blood group antigens (HBGAs) present throughout many parts of the body, yet primarily causes disease in the gastrointestinal tract (Almand, Moore, & Jaykus, 2017; J. Le Pendu, 2004). As glycan motifs such as fucosylated *N*-glycans or fucosylated LacNAcs (LNFs) are often shared across many species, however, these motifs still differ in their levels of expression even between tissues within the same species (Gagneux & Varki, 1999; Varki, 2006, 2017). Therefore, viruses such as MrNV that exhibit broad species and tissue infectivity, yet specific in tissue pathogenesis may reflect the aforementioned concept. Regarding the dependence on glycans for host interaction in the nodavirus family, the binding of the Dragon grouper nervous necrosis virus (DGNNV) VLPs, a betanodavirus closely related to the Malabar grouper nervous necrosis virus (MGNNV), was shown to be highly sensitive to the treatment of SSN-1 fish cell lines with tunicamycin and neuraminidase (Liu et al., 2005; Low, Syarul Nataqain, Chee, Rozaini, & Najiah, 2017). This report was the first study to demonstrate the

importance of *N*-glycosylation and interestingly sialic acids in the binding and internalization process of a nodavirus. The involvement of glycans in the nodavirus infection process was further demonstrated in grouper per fin cell lines (GF-1), in which it was proposed that the nervous necrosis viruses interacted with the heat shock cognate protein 70 (Hsc70) near the cell surface. Hsc70 in turn purportedly further interacts with GF-1 surface glycosaminoglycans (GAGs), facilitating attachment and internalization of the virus particles (Chang & Chi, 2015; Low et al., 2017). MrNV may thus be similar to many other viruses, both enveloped and non-enveloped, that are dependent on glycans for the initial binding and internalization into host cells.

In regard to other non-enveloped viruses, especially members of the ssRNA+, *Caliciviridae* and *Picornaviridae* depend on specific host surface glycan motifs for susceptibility and cell attachment factors. Noroviruses of the *Caliciviridae* rely on interactions with fucosylated human blood group antigens (HBGAs), depending on the strains. On the other hand, the ssRNA+ *Picornaviridae* viruses are dependent on sialylated receptors, in particular α 2, 6-linked neuraminic acid (Neu5Ac)-containing glycans (Ashok & Atwood, 2006; Stencel-Baerenwald, Reiss, Reiter, Stehle, & Dermody, 2014; Stroh & Stehle, 2014). Furthermore, other non-enveloped viruses such as members of the dsDNA *Reoviridae* that infect hosts ranging from mammals to insects depend on glycans found in HBGAs or NeuAc-terminated glycans. Finally, the non-enveloped members of the ssDNA *Parvoviridae* along with members of the *Papovaviridae* are both dependent on glycosaminoglycans in the form of heparan sulfate for binding and cell entry (Huang, Halder, & Agbandje-McKenna, 2014; Raman, Tharakaraman, Sasisekharan, & Sasisekharan, 2016; Shanker et al., 2017; Stencel-Baerenwald et al., 2014; Stroh & Stehle, 2014; Thompson, de Vries, & Paulson, 2019).

Accordingly, the we aimed to elucidate the role of glycans as host-surface binding molecules that specifically interact with MrNV-VLPs. Therefore, the present study

demonstrates for the first time the dependence of MrNV, in the form of virus-like particles (MrNV-VLPs), on glycans present in the gills of the giant freshwater prawn *M. rosenbergii*. Furthermore, we also report the identification of unique fucosylated LacdiNAc-extended (LDNF) *N*- and *O*-glycans, and that the VLPs were more dependent on *N*-linked than on *O*-linked fucosylated glycans for binding to gill proteins. Thus, these findings help to elucidate the putative binding factors of MrNV in host tissues, and should facilitate the development of infection-blocking strategies based on the virus-glycan interactions as revealed in this study.

RESULTS

Gill tissues are the initial binding site of MrNV-VLPs

The general binding ability of the virus-like particles of M. rosenbergii nodavirus (MrNV-VLPs) to various tissue lysates of *M. rosenbergii* was shown by ELISA (Fig. 1A). To identify which tissue was the initial site of binding for MrNV-VLPs, we conducted whole-mount immunohistochemistry. MrNV-VLPs were pre-conjugated with NHS-X-biotin for labeling, and then tracked using Alexa 488-conjugated avidin, an approach preferred over a primary/secondary antibody approach due to inefficient perfusion of the probes into the tissues. When post-larval stage *M. rosenbergii* were immersed with biotin-conjugated MrNV-VLPs over a three-day period, the particles mainly localized in the gills as shown by the strong green fluorescence (Fig. 1B). This was further confirmed when gill tissue sections incubated with MrNV-VLPs showed extensive binding of the particles throughout the gill lamellae, which can be clearly observed by the red fluorescence on the lamellar epithelial lining (LEL) and the internal pillar cells (PC) of the gills (Fig. 1C, row 2, panel 3). This level of epithelial binding was neither observable in the hepatopancreas tissue sections nor in the muscle tissue sections (Sup. Fig. 1). Accordingly, these observations suggested the gills were the initial binding site upon exposure to MrNV-VLPs.

151

152 **MrNV-VLP binding to gill tissues is glycan-dependent**

153 The possibility of glycans being involved in the binding process of MrNV-VLPs to the
154 gills was examined using chemical and enzymatic methods, either on protein lysates or tissue
155 sections. Treatment with sodium metaperiodate ($NaIO_4$), which disrupts the intact structures of
156 glycans, resulted in the highest level of reduction of MrNV-VLP binding to gill tissue lysates.
157 In addition, treatment with the *N*-glycan core digesting enzyme PNGase F caused a significant
158 reduction in particle binding but at a lower level than that of $NaIO_4$ (Fig. 2A). However, it was
159 also possible that the enzyme was either not able to totally remove all *N*-glycans represented
160 by residual levels of GlcNAcs detected by sWGA, or that the lectin was also detecting terminal
161 GlcNAcs of *O*-glycans (Fig. 2B). Additionally, the treatments with the glycosidases α1-2,3,6
162 mannosidase, and α1-2,3,4,6 fucosidase both caused moderate reductions in MrNV-VLP
163 binding (Fig. 2A), even though not being able to totally digest all mannoses and fucoses from
164 the lysates (Fig. 2B). As a result, the glycosidases were still able to reduce MrNV-VLP binding
165 levels in direct proportion to the level of digestion as shown in Figure 2B. These results, thus,
166 demonstrated that the binding MrNV-VLPs to gill tissue lysate glycans were sensitive to
167 reductions in total glycans by $NaIO_4$, reductions of *N*-glycans levels by PNGase F, and to
168 partial digestions of mannosylated and fucosylated structures.

169 The reduction of MrNV-VLP binding due to alterations in glycan levels by $NaIO_4$ and
170 PNGase F was further examined in gill tissue sections. As shown in Figure 2C, gill tissues
171 exhibited a high level of Con A and sWGA staining throughout the lamellar folds (GL), and in
172 particular the lamellar epithelial lining (LEL), the pillar cells (PC) and the gill tips (GT) where
173 gaseous exchange takes place. These observations suggested that the epithelial lining and cells
174 possessed glycans that were both mannose and GlcNAc-rich. When the tissue sections were
175 incubated with $NaIO_4$ and PNGase F, there were evident, significant reductions of the green

fluorescence representing Con A and sWGA staining, respectively, along the epithelium (Fig. 2D, 3rd column.); hence, indicating a reduction in glycans. The reductions in green fluoresecence of the lectins in the $NaIO_4$ and PNGase F-treated sections corresponded to a near total inhibition of MrNV-VLP binding as evidenced by nearly absent red fluorescence (Fig. 2D, rows 2 and 3, 4^{th} column). Consequently, these epifluorescence microscopy results and ELISA experiments showed the MrNV-VLPs' dependence on glycans of the gill tissues for binding.

Gill tissue presents unique fucosylated *N*- and *O*-glycans

Considering the involvement of glycans for the binding of MrNV-VLPs to gills, we further examined glycosylation patterns in order to identify possible glycan targets. Composition analysis by gas chromatography was conducted on major tissues to provide a general picture of the predominant carbohydrates present in the selected tissues. The results showed the presence of galactose (Gal), mannose (Man), fucose (Fuc), *N*-acetylgalactosamine (GalNAc) and *N*-acetylglucosamine (GlcNAc) residues in variable proportions (Sup. Fig. 2). Observation of high proportion of Man indicates the presence of oligomannosylated *N*-glycans, whereas Gal, Fuc, GalNAc and GlcNAc may be part of complex *N*- and *O*-glycans. Of particular interest, we note the high ratio of Fuc:[GlcNAc+Gal] in the gill (1.5) compared to that in muscle (0.4) and in the hepatopancreas (0.7) that is indicative of abundant fucosylated epitopes, possibly Lewis-type in this very tissue. Finally, in agreement with the accepted absence of sialic acids in Arthropoda (Tiemeyer, Nakato, & Esko, 2015), no sialic acid derivative could be identified in these tissues.

We further attempted to pinpoint the major *N*- and *O*-glycans present in the gill tissue to further examine the specific glycosylation patterns involved in MrNV-VLP binding. Accordingly, gill tissue lysates were processed to release and enrich *N*- and *O*-glycans, then

subjected to MALDI-MS and MS/MS analyses. The *N*-glycan profile revealed a complex pattern dominated by the signal at *m/z* 2396.3 assigned to $[M+Na]^+$ adduct of $Man_9GlcNAc_2$ oligomannosylated *N*-glycan, along with a signal at *m/z* 2192.2 assigned to $Man_8GlcNAc_2$, in accordance with the prevalence of Man in the monosaccharide composition (Fig. 3A). The other three major signals at *m/z* 1590.9, 2010.1 and 2674.4 were annotated as $Fuc_1Hex_3HexNAc_3$, $Fuc_2Hex_3HexNAc_4$ and $Fuc_3Hex_3HexNAc_6$, respectively. MALDI-MS/MS spectrum of signal at *m/z* 2010 showed the presence of a Fuc residue both at the terminal reducing HexNAc residue owing to the fragment ion at *m/z* 1558 and on the non-reducing $HexNAc_2$ branch according to the fragment ion at *m/z* 1331 (Sup. Fig. 3). The last Fuc residue could be positioned at the C3 position of the internal HexNAc residue owing to the combined Y fragment ions at *m/z* 1750 and Z fragment ion at *m/z* 1883, which defines the terminal HexNAc(Fuc-3)HexNAc glycotope. Altogether, these data strongly suggest the presence of *N*-glycans sharing a core fucosylated structure differentially extended by HexNAc, HexNAc(Fuc)HexNAc, and $[HexNAc(Fuc)HexNAc]_2$ motifs, respectively. These glycotopes are highly reminiscent of LacdiNAc (GalNAcβ1-4GlcNAc) epitopes synthesized by insects and other invertebrates in place of LacNAc (Galβ1-4GlcNAc) more commonly observed in vertebrates.

The MS profile of *O*-glycan revealed four major signals at *m/z* 953.4, 994.5, 1127.5 and 1168.5 which were annotated with $Fuc_1Hex_1HexNAc_1$-HexNAcitol, $Fuc_1HexNAc_2$-HexNAcitol, $Fuc_2Hex_1HexNAc_1$-HexNAcitol, and $Fuc_2HexNAc_2$-HexNAcitol, respectively (Fig. 3B). MS/MS analyses of these four signals indicated that these are Core 3 based *O*-glycans extended with different variations of fucosylation on gill tissue (Fig. 3C-F). MS/MS spectra of $[M+Na]^+$ molecular ions at *m/z* 953 and 1127 showed that the respective terminal glycotope is type-1 H glycotope based on C ion at m/z 433 and Z ion at m/z 543 (Fig. 3C), and Lewis b glycotope based on B ion at *m/z* 834 and Z ion at *m/z* 717 (Fig. 3E). MS/MS spectra

of another two signals at *m/z* 994 and 1168 showed the presence of an LDNF chain according to B ion at *m/z* 701 (Fig. 3D) and B ion at *m/z* 875 (Fig. 3F). Additionally, the respective Z ion at *m/z* 788 (Fig. 3D) and *m/z* 962 indicated the terminal glycotopes are HexNAc(Fuc-3)HexNAc and (Fuc3-)HexNAc(Fuc-3)HexNAc. This LDNF chain is present on *N*-glycans as well. Therefore, the major *O*-glycans identified in the gill tissues appeared to be unique fucosylated glycans. The possibility of their interactions with MrNV-VLPs was explored in subsequent experiments.

The fucose-binding *Aleuria aurantia* lectin (AAL) blocks the specific interaction between and MrNV-VLPs and gill tissue proteins

To examine if MrNV-VLPs interact specifically with fucosylated glycoproteins of the gills, pull-down assays and Far Western blotting were performed using the particles as bait and the gill proteins as prey proteins. Firstly, Coomassie staining of SDS-PAGE gels of the gill proteins showed bands with masses ranging from 15 kDa to 250 kDa (Fig. 4 panel 1, lane 1). The gill proteins (prey) that interacted specifically to MrNV-VLPs (bait) were obtained by passing total gill protein lysates through VLP-coated columns (pull-down assay), and the eluted gill proteins were subjected to SDS-PAGE. The gel showed that the gill proteins that interacted with the VLPs had weights of between ~65 and ~75 kDa (Fig 4A, panel 1, lane 3). The co-eluted MrNV-VLPs appeared as a fainter band at ~42 kDa (Fig 4A, panel 1, lane 2). To further confirm that the MrNV-VLPs did specifically interaction with the ~65-~75 kDa bands of the gill proteins, we performed Far Western blotting. PVDF membranes with transferred gill proteins that underwent the pull-down assay were incubated with MrNV-VLPs again as the bait protein and detected by anti-6xHis antibodies. The Far Western blot results showed that the MrNV-VLPs did bind strongly to the the ~65-75 kDa bands of the gill proteins from the pull-down assay (Fig. 4, panel 2, lane 3 upper band), and this selective binding was further

confirmed by the MrNV-VLPs binding at the same ~65-75 kDa bands in the crude gill protein lane (Fig. 4, panel 2, lane 1). In Western blots using the AAL lectin as a probe revealed a binding to a large number of bands in the lane of crude gill proteins (Fig. 4, panel 3, lane 1), and to the ~65-~75 kDa bands of the pull-down gill protein lane (Fig. 4, panel 3, lane 3). When the membrane was pre-incubated with AAL, there was nearly a complete blocking of MrNV-VLPs binding to crude gill protein lane (Fig. 4, panel 4, lane 1), and the same was observed in the pull-down gill protein lane (Fig. 4, panel 4, lane 3). Therefore, these results further confirmed that the MrNV-VLPs selectively interacted with fucosylated glycoproteins of the gills, as evidenced by the MrNV-VLPs binding to both pull-down and crude gill proteins of similar MW, and the disruption of this interaction by the broadly specific fucose-binding AAL.

MrNV-VLPs binding to gill tissues is blocked by fucose-binding lectins

To further verify the MrNV-VLP interaction with gill proteins were dependent on fucosylated glycoproteins, a panel of lectins were used to examine if there were other glycotopes also involved in the binding process. The ELISA experiments showed that the AAL lectin still showed the most inhibition (over 75%) of MrNV-VLPs binding to gill protein lysates (Fig. 5A). BC2L-C-Nt, which recognizes H-type 1, Le^b, and Le^y antigens, nor UEA-I, which recognizes primarily H-type 2 antigen displaying glycoconjugates, displayed efficient inhibition ability. However, Con A, which recognizes glycoconjugates containing high mannose type, hybrid type and bi-antennary *N*-glycans caused nearly a one-fold reduction in binding. Furthermore, sWGA that recognizes GlcNAcs caused a significant but small reduction, while LCA which binds to core-fucosylation of *N*-glycans did not exhibit any significant inhibition. On the other hand, PNA which binds to *O*-glycan LacNAcs (Tn-antigen) caused a significant but low level of inhibition, while RCA-I that binds to galactose/GalNAc and AIA (sialylated Tn-antigens) were ineffective.

When the gill tissues were pre-incubated with AAL, the lectin staining could be observed as an intense, green fluorescence throughout the gill tissue especially the lamella (GL) (Fig. 5B, row 5 panel 3). Simultaneously, there was a near complete loss of MrNV-VLP binding to the gill tissues when gill tissues were pre-incubated with AAL (Fig. 5B, row 5 panel 4), similar to that observed following sodium metaperiodate treatment (Fig. 1C row 2). On the other hand, pre-incubation of the gill tissues with BC2L-C-Nt and Con A resulted in a moderate inhibition of MrNV-VLP binding (Fig. 5B, rows 2 and 3). Neither the *N*-glycan binding LCA nor the *O*-glycan binding PNA caused any reductions (Fig. 5B, rows 4 and 6). Other lectins such as UEA-I, RCA-I, WGA, AIA and PhosL (results not shown) also did not cause noticeable effects on binding.

MrNV-VLPs prefer fucosylated *N*-glycans over *O*-glycans for binding

In earlier results, the PNGase F treatment reduced MrNV-VLP binding to gills extracts and tissues, suggesting the involvement of *N*-glycans (Fig. 2A). To further examine whether MrNV-VLPs interact specifically with *O*-glycans, gill tissue lysate-coated wells were treated with a GlycoProfile β-Elimination Kit to reduce total *O*-glycan levels (efficiency of *O*-glycan reduction shown in Sup. Fig. 4). Interestingly, the reduction of *O*-glycan by beta-elimination resulted in more than a two-fold increase in the binding of the VLPs to the tissue lysates (Fig. 6). This could either indicate that the reagent reduced *O*-glycan complexities which further increased exposure to the *O*-glycans for binding, or there was increased access to fucosylated *N*-glycans. To verify the latter notion, we again used the Con A, AAL and BC2L-C-Nt lectins to try and block VLP binding after treatment with the beta-elimination reagent. The results showed that Con A reduced virus particle binding by nearly one-fold compared to reagent-treated lysates, and more notably AAL was able to reduce binding to levels lower than those of both reagent and non- treated lysates. BC2L-C-Nt, PNA and UEA-I which served as *O*-

glycan-blocking lectins did not affect binding levels significantly (Fig. 6). Therefore, in conjunction with the effects of PNGase F of earlier results, the reduction in MrNV-VLP binding by these lectins after beta-elimination supported the notion that the reduction of *O*-glycan levels more likely increased access for the binding of MrNV-VLPs to fucosylated *N*-glycans.

MrNV-VLPs exhibit binding to immobilized fucosylated glycoconjugates

As the gill tissue lysates involved a large mixture of glycans from a crude extract, we coated immobilized glycans with known structures onto ELISA wells in order to pinpoint more precisely the carbohydrate moieties or motifs recognized by the MrNV-VLPs. With the selected panels of glycans used, MrNV-VLPs showed the highest level of binding towards polyacrylamide-conjugated alpha-fucose (PAA-α-Fucose), followed by PAA-GlcNAc, PAA-Gal, and PAA-GalNAc (Fig. 7); thus, confirming their preference for fucosylation.

Furthermore, MrNV-VLPs showed some levels of binding to the more complex fucosylated Lewis antigens, in particular human serum albumin-conjugated Lewis a (HSA-Le^a) (Fig. 7). Therefore, these immobilized glycoconjugate results further confirmed the earlier experiments that the MrNV-VLPs preferred fucosylated glycans in general, and the moderate levels of binding to the Lewis antigens may reflect the nature of their broad specificity.

DISCUSSION

The Macrobrachium rosenbergii nodavirus (MrNV) is a non-enveloped virus, which, as we have demonstrated in a previous study, is highly dependent on the C-terminal 26 amino acids of the protruding P-domains for the binding and interaction process with the permissive Sf9 insect cell line (Monsicha Somrit et al., 2017). In our present study, we describe for the first time in this species that MrNV in the form of virus-like particles (VLPs) is highly

dependent on fucosylated glycans as binding factors on giant freshwater prawn tissues and that glycan-removal/blocking agents such as periodate, glycosidases and lectins could affect binding levels. Furthermore, this study also revealed the existence of *N*- and *O*-glycans with unique structures in the gill tissues, which may lead to the development of compounds that can specifically block viral attachment.

We demonstrated through the wholemount technique that the MrNV-VLPs attach primarily to the gill tissues of the post-larvae specimens. Past studies using *in situ* hybridization in diseased post-larval (PL) stage of prawn showed that the localization of MrNV were mainly in the striated muscles of the abdomen, cephalothorax and appendages (Sahul Hameed et al., 2004; Sri Widada et al., 2003). Some studies showed that some signals of the virus can be found in the gills (Jean-Michel et al., 1999), and either in the intertubular epithelial cells or the phagocytic hemocytes within the hepatopancreas (Hsieh et al., 2006). The differences between the localization in our study using non-replicating VLPs and the aforementioned reports using infectious MrNV inocula may be explained by the fact that MrNV signals in past studies were observed only after the disease had progressed long enough for pathological signs of WTD to be noticeable (Hsieh et al., 2006; Sri Widada et al., 2003). As such, the detection in muscle tissues of the virus-afflicted specimens may reflect the "terminal" stage of the disease and does not provide information about the initial entry points of exposure/infection to the virus. The use of MrNV-VLPs as in our study, while not causing viral infection and pathologies in the susceptible host tissues, still provided a simple and meaningful way to observe the virus binding process due to their structural homology with native MrNV. Additionally, the wholemount experiments showing high level of MrNV-VLP binding to the gill tissues of PL may better reflect the natural introduction of the virus into the prawns incompletely closed circulatory system (McGaw, 2005).

The gills of decapod crustaceans are involved in gaseous exchange, in maintaining osmotic and ionic balance, in excretion/detoxification and in the immune response towards invading pathogens (Felgenhauer, 1992; Freire, Onken, & McNamara, 2008). With gaseous exchange requiring the oxygenation of hemocyanin within the hemolymph and conveyed to all tissues by the arterial system (Henry, Lucu, Onken, & Weihrauch, 2012), the gills can provide a quick route for the entry of viral pathogens to ultimately cause infections in tissues throughout the animal. Our results showing the preference of MrNV-VLPs for the gills may indicate the potential exploitation of the tissue by the virus as a point of entry and transfer. This notion is supported by past studies showing that an influx of hemocytes in the gills occurs in *M. rosenbergii* challenged with pathogens (Jayasankar et al., 2002; Okuno et al., 2002), and that hemocytes can be and remain infected with MrNV after they have migrated to distant tissues (Gangnonngiw, Bunnontae, Phiwsaiya, Senapin, & Dhar, 2020; Hsieh et al., 2006). Therefore, our wholemount results demonstrated the gills as the initial tissues for MrNV-VLP binding, but further studies are required to characterize the transmission of the virus between the gills and hemocytes that ultimately results in infection of the muscles.

The surface binding factors for MrNV in susceptible cells or tissues of *M. rosenbergii* have yet to be fully elucidated. A recent study has shown cell surface-interacting transglutaminase (MrTGII) to be important in the binding and internalization process into *M. rosenbergii* hemocyte cells. MrTGII, and transglutaminases in prawn in general, are involved in the hemocyte clotting process during bacterial infections. Furthermore, through the existence of RGD-domains in MrTGII, and the fact that transglutaminases in vertebrates interact with the GAG heparan sulfate, it has been proposed that the enzyme may interact with cell surface integrins and GAGs to facilitate the entry of MrNV into the hemocytes (Gangnonngiw et al., 2020). While these findings are preliminary and require further studies, it does indicate the possibility of glycans as facilitating factors in the binding process of MrNV. Previous studies

375 also revealed the potential role of glycans as binding factors for the *Alpha* and *Beta* genera of
376 nodaviruses, our study adds a *gammanodavirus* to the list of glycan-binding nodaviruses.

377 Following the demonstration that tissue glycans were crucial for the binding of the virus
378 particles, we have established the structures of *N*- and *O*-glycans from gill in order to identify
379 unique glycan structures that may be targeted by MrNV for binding. The *N*-glycan profiles
380 revealed three major signals, all of which shared a core fucosylated structure and differentially
381 extended by HexNAc, HexNAc(Fuc)HexNAc, and [HexNAc(Fuc)HexNAc]$_2$ motifs,
382 respectively. While the core fucosylated structure of the *N*-glycans is ubiquitous, the α1-3
383 fucosylation is typically found in invertebrates (Paschinger & Wilson, 2019). However, in this
384 study, the ability of PNGase F to significantly reduce both the levels of glycans and MrNV-
385 VLP binding in the gill tissue sections and lysates strongly suggested that the N-glycan core
386 was fucosylated at the α1-6 position.

387 HexNAc extended core-fucosylated structures are similar to the "pseudohybrid",
388 paucimannosidic *N*-glycans found in the *Drosophila melanogaster* and *Caenorhabditis elegans*
389 N-glycomes (Leonard et al., 2006; North et al., 2006; Schachter, 2009). Furthermore, the
390 biantennary core fucosylated-HexNAc glycan structure was also found as part of the *N*-
391 glycome of the lepidopteran cell lines Sf-21 and Bm-N (Kubelka et al., 1993), in glycoproteins
392 expressed from *Trichoplusia ni* cells (Hsu et al., 1997), in the nematode *Pristionchus pacificus*
393 (Yan, Wilson, & Paschinger, 2015), and in larvae of several dipteran species (Kurz et al., 2015).
394 On the other hand, the HexNAc(Fuc)HexNAc, and [HexNAc(Fuc)HexNAc]$_2$ *N*-glycan motifs
395 are both biantennary fucosylated LacdiNAc (LDNF) structures extended from the fucosylated
396 core, both structures of which, while not unique, are specifically found in only a handful of
397 organisms till date. LacdiNAc (LDN), and in particular LDNF, are motif extensions found
398 almost exclusively in invertebrates and highly immunogenic in mammalians where the
399 LacNAc extension is more predominant (van Die & Cummings, 2010). The single-branched

HexNAc(Fuc)HexNAc extension of the core was observed in the *N*-glycomes of the lepidopteran *T.ni* and *Lymantria dispar* larvae (Stanton et al., 2017), the ruminant-afflicting nematode *Haemonchus contortus* (Paschinger & Wilson, 2015), in a sulfated form of the dipteran *Anopheles gambiae* (Kurz et al., 2015; Kurz, King, Dinglasan, Paschinger, & Wilson, 2016), the egg/miracidia stages of helminthic parasite *Schistosoma mansoni* (Smit et al., 2015) and in the nematode *Dirofilaria immitis* (Martini et al., 2019). The HexNAc(Fuc)HexNAc extension bound with phosphoethanolamine (PE) was also found in the *N*-glycomes of the male larvae and venom of *Apis mellifera,* and can be further extended with βGal or α/βGalNAc (Hykollari, Malzl, Stanton, Eckmair, & Paschinger, 2019; Kubelka et al., 1993; Rendić, Wilson, & Paschinger, 2008).

The biantennary $[HexNAc(Fuc)HexNAc]_2$ *N*-glycan motif in this exact form has been previously reported in 6-week-old worms of *S. mansoni* whose N-glycome was otherwise dominated by biantennary fucosylated LacNAcs (Lewis x-like extensions) (Prasanphanich, Mickum, Heimburg-Molinaro, & Cummings, 2013; Smit et al., 2015). These LDNF glycotopes have been shown to elicit a strong immune response in the host animal towards *S. mansoni* (Prasanphanich et al., 2014; Prasanphanich et al., 2013). Similar biantennary motif extensions with additional βGal-βGlcA or with terminal fucosylations have been shown in the glycomes of *A. mellifera* (Hykollari et al., 2019; Rendić et al., 2008) and in *D. immitis* (Martini et al., 2019), respectively.

The four glycan structures identified in the gill *O*-glycome were fucosylated, core 3 mucin-type *O*-glycans which are unique structures that have not so far been reported in invertebrate *O*-glycomes (Staudacher, 2015; Walski, De Schutter, Van Damme, & Smagghe, 2017; Zhang & Ten Hagen, 2019; Zhu, Li, & Chen, 2019). Of the four identified *O*-glycans in our study, the first and the third were essentially fucosylated LacNAcs; the first corresponding to the H-type 1 glycotope (Fucα1-2Galβ1-3GlcNAc) and the third determined to be a Lewis b

425 glycotope (Fucα1-2Galβ1-3(Fucα1-4)GlcNAc). Both the H-type 1 and Lewis b are glycotopes
426 of the HBGA system and have been demonstrated to be specific ligands for strains of
427 noroviruses and rotaviruses, which are enteric viruses belonging to the *Caliciviridae* and
428 *Reoviridae* family, respectively (Jacques Le Pendu & Ruvoën-Clouet, 2019). The two
429 remaining identified *O*-glycans (second and fourth) were both fucosylated LacdiNAcs (LDNFs)
430 linked to the core *O*-GalNAc, which are unique structures for *O*-glycans in invertebrates that
431 mostly display branching LacNAc or βGal from the *O*-GalNAc core (Staudacher, 2015). A
432 single study reported through structural analysis and antibody reactivity the presence of Le^x
433 substituted *O*-glycans in salivary mucins of the wasp *Vespula germanica* (Garenaux, Maes,
434 Leveque, Brassart, & Guerardel, 2011), It is also notable that the LDNF extensions to the *O*-
435 GalNAc core of the two of four *O*-glycans in this study highly resemble the LDNF antennary
436 extensions in the *N*-glycans described earlier in the study. Thus, the LDNFs and the fucosylated
437 glycans found in the *N*- and *O*- glycomes in the gill tissues were the primarily candidates as
438 binding factors for MrNV.

439 Previous studies have shown that MrNV can bind, infect and successfully replicate in
440 the dipteran (*Aedes albopictus*) cell line C6/36 (Hayakijkosol & Owens, 2013) and lepidopteran
441 (*Spodoptera frugiperda*) cell line Sf9 (M. Somrit et al., 2016). Interestingly, recent studies in
442 several species of dipterans closely related to *A. albopictus*, including *Aedes egyptii* and *A.*
443 *gambiae* reported that their *N*-glycomes contained LDNF core extensions with the presence of
444 additional terminal βGal or βGlcA residues (Kurz et al., 2015; Kurz et al., 2016). Similarly, the
445 *N*-glycomes of lepidopterans such as Sf21 cells, *T.ni* cells, High Five cells, and *L. dispar*
446 showed varying levels of LDNFs similar to the *N*-glycan identified in our MALDI-TOF
447 MS/MS results, but with minor additions (Kubelka et al., 1993; Rendić et al., 2008; Stanton et
448 al., 2017) (see a comparison in Sup Fig. 5). However, no similarities can be drawn between
449 dipteran/lepidopteran *O*-glycans with those identified in the *M. rosenbergii* gill tissues. The *O*-

glycomes of dipterans appear to be dominated by core 1 mucin-type *O*-glycans, with additional glucuronic acids or fucosylations (Kurz et al., 2015; Staudacher, 2015; Walski et al., 2017). The *O*-glycome of Sf9 cell line showed the presence LacNAc and LacdiNAc extensions to the *O*-GalNAcs but without fucosylation (Gaunitz et al., 2013; Walski et al., 2017).. Therefore, the marked similarities between the fucosylated LacdiNAcs *N*-glycans but not *O*-glycans identified in the gill tissues of the *M. rosenbergii* and those identified in dipteran and lepidopteran cell lines known to be susceptible to MrNV infection may suggest the possibility of fucosylated *N*-glycans as being the common binding factor for this virus.

The importance of fucoyslated glycans in MrNV-VLP binding to gill tissues was further confirmed by the use of fucose-binding lectins. As shown in the lectin-blocked tissue sections and tissue lysate experiments, incubation with the AAL lectin caused the highest level of reduction of MrNV-VLP binding as compared to other fucose-specific lectins in LCA, BC2L-C-Nt and UEA-I. Given that AAL is a lectin that has been shown to bind to α1-2,3,4, or 6 fucosylations in particular those bound to GlcNAc-containing glycans (Bergstrom, Astrom, Pahlsson, & Ohlson, 2012; Matsumura et al., 2007; Wimmerova, Mitchell, Sanchez, Gautier, & Imberty, 2003), it was highly likely that the lectin was capable of binding to the *N*-linked/*O*-linked LDNF extensions or even the core fucosylation of the gill glycans. However, lack of significant blocking by LCA or the more specific PhoSL (data not shown) suggested the VLPs' low preference for the core α1-6-linked fucose for binding. Furthermore, the relatively low blocking levels by BC2L-C-Nt and UEA-I suggested that terminal α1-2-linked terminal fucoses, which are the targets of both lectins (Baldus et al., 1996; Sulak et al., 2011), along with H-type 1/2 or Lewis b/y antigens were highly unlikely to be involved.. The dependence on fucosylated glycans was further confirmed by the Western blot experiments, in which the AAL lectin interacted specifically with the 65-75 kDa bands of gill proteins from the pull-down assays. Moreover, the pre-incubation of the PVDF membranes with AAL abolished MrNV-

475 VLP binding to both crude and pull-down proteins, thus, confirming the capability of AAL in
476 blocking the binding of the particles to fucosylated glycoproteins present in the gill tissues.
477 In conjunction with the PNGase F results, the ability of the Con A lectin to reduce
478 MrNV-VLP binding better than *O*-glycan binding lectins such as PNA and AIA suggested that
479 *N*-linked glycans were the main type of glycosylation involved in the binding process.
480 Furthermore, mannose residues may be directly or indirectly involved in interaction of MrNV-
481 VLPs with the LDNF extensions. These results were further supported by the treatment of the
482 gill protein lysates with beta-elimination reagent. Although the removal of *O*-glycans by the
483 reagent was not complete (Sup. Fig. 4), it was evident that beta-elimination of the gill lysates
484 resulted in a significant increase in MrNV-VLP binding. This led us to question whether this
485 was the effect of the reduced complexities of the *O*-glycan or an increased exposure of *N*-
486 glycans that may have facilitated more particle binding. Subsequently, beta-elimination
487 reagent-treated gill proteins were then incubated with Con A and AAL to block remaining
488 exposed *N*-glycans; while PNA, UEA-I and BC2L-C-Nt used for the remaining *O*-glycans.
489 Ultimately, incubations with Con A and AAL resulted in the reduction of MrNV-VLP binding
490 levels equal or even below that of untreated gill protein, strongly suggesting that the virus
491 particles had a preference for fucosylated *N*-glycans over the *O*-glycans.
492 In the present study, we demonstrated for the first time that fucosylated glycans, and in
493 particular those of the *N*-glycan type, can act as factors that facilitate the binding and interaction
494 process of MrNV-VLPs with the gill tissues of the giant freshwater prawn *M. rosenbergii*.
495 Furthermore, mass spectrometry revealed the existence of *N*- and *O*-glycans with unique LDNF
496 structures in the gills, which correspond well with the other results that show the high
497 preference of the non-infectious MrNV-VLPs for gill tissues and fucosylated *N*-glycans.
498 Therefore, the knowledge gained from the present study using the VLP counterpart of the
499 infectious, native MrNV should lead to a better understanding of the dependence of the virus

on fucosylated *N*-glycans for binding and interaction in susceptible tissues such as the gills and also lead to the development of either fucosylated glycan-based or fucosylated glycan-targeting compounds in order to combat viral infection.

EXPERIMENTAL PROCEDURES

Chemicals and reagents

The tryptone and yeast extract used for preparing Luria Bertani (LB) broth were purchased from Titan Biotech, Delhi, India. Sodium chloride (NaCl), sodium carbonate (Na_2CO_3) sodium bicarbonate ($NaHCO_3$), iodoacetamide (IAA), aminopropylsilane, sulfosuccinimidyl-6-(biotinamido)hexanoate (NHS-X-biotin), glycine, goat anti-mouse horseradish peroxidase (HRP), polyvinylidene fluoride (PVDF) blotting membranes, sodium hydroxide (NaOH) methanol, chloroform, pyridine, hydrochloric acid, formic acid, ethylenediaminetetraacetic acid (EDTA) and 4′,6-diamidino-2-phenylindole dihydrochloride (DAPI) were purchased from EMD , Darmstadt, Germany.

Ampicillin hydrochloride, Tris hydrochloride, imidazole, isopropyl β-d-1-thiogalactopyranoside (IPTG), sodium phosphate monobasic/dibasic, fraction V bovine serum albumin (BSA) were purchased from Vivantis Technologies, Subang Jaya, Malaysia. Trypsin, chymotrypsin, glucose, mannose, β-*N*-acetylglucosamine (β-GlcNAc), L-fucose, α-galactose, β-*N*-acetylgalactosamine, (β-GalNAc), sialic acid, mouse anti-hexahistidine tag monoclonal antibodies, sodium metaperiodate, Triton-X 100, Tween 20, sodium borohydride, dichloromethane, GlycoProfile β-Elimination Kit and porcine mucin were purchased from Sigma-Aldrich, MO, USA. Alexa 488/594-conjugated goat-anti-mouse antibodies and Alexa 488-conjugated avidin were purchased from Thermo Fisher Scientific, MA, USA.

PNGase F, α1-2,3,6 mannosidase, and α1-2,3,4,6 fucosidase were purchased from New England Biolabs, MA, USA. Biotinylated lectins concanavalin A (ConA), succinylated

wheatgerm agglutinin (sWGA), *Lens culinaris* agglutinin (LCA), peanut agglutinin (PNA), *Ricinus communis* agglutinin I (RCA-I), *Artocarpus integrifolia* agglutinin/Jacalin lectin (AIA), *Ulex europeaus* agglutinin I (UEA-I), *Aleuria aurantia* lectin (AAL), and *Lotus tetragonolobus* lectin (LTA) were purchased from Vector Labs, CA, USA. Biotinylated BC2L-C-Nt, biotinylated PhosL, human serum albumin-conjugated (HSA) glycans (Isosep, Tullinge, Sweden), and polyacrylamide-conjugated (PAA) glycans were kind gifts from Drs. Anne Imberty and Annabelle Varrot (CNRS, Grenoble, France) and Dr Nicolai Bovin (IBCh RAS, Moscow, Russia), respectively.

Preparation of Macrobrachium rosenbergii Nodavirus virus-like particles (MrNV-VLPs)

Recombinant MrNV capsid proteins were expressed and purified according to previously described methods (Jariyapong et al., 2014). Briefly, pET16b plasmids (Novagen, Darmstadt, Germany) containing an inserted MrNV capsid protein gene with hexahistidine tag sequence (MrNVCAP-6xHis) were transformed into competent *E. coli* BL21 (DE3). The bacterial culture was then inoculated into LB broth containing 50 μg/mL of ampicillin, induced with 1 mM IPTG (25°C, 3 hr) and lysed in phosphate-buffered saline (PBS) containing protease inhibitor cocktail (GE Healthcare, Piscataway, NJ). The lysate supernatant was filtered and applied onto a Ni-NTA Histrap HP column. The MrNV-VLPs fractions were eluted by elution buffer (20mM Tris-HCl, 250 mM imidazole, 500 mM NaCl, pH 7.4) and then desalted with a G25 desalting column (GE Healthcare, Piscataway, NJ, USA).

Examination of binding levels of MrNV-VLPs to post-larvae wholemounts, and to disease-associated tissues using ELISA and immunohistochemistry

The *M. rosenbergii* post-larvae specimens were fixed with 4% paraformaldehyde overnight. The fixed post-larvae were decalcified in 0.1 M hydrochloric acid/formic acid for 3 days at room temperature, then washed extensively with PBS solution. To prepare fluorescence-conjugated MrNV-VLPs for wholemounts, 1 mg of MrNV-VLPs in 500 μl PBS

pH 7.4 were mixed with a 1 mM solution of NHS-X-biotin. The decalcified shrimp were incubated in a 20 μg/mL solution of biotinylated-MrNV-VLPs for 2 days, followed by another 2-days incubation in Alexa 488-conjugated avidin and DAPI before being visualized under an epifluorescence microscope.

Giant freshwater prawn *M. rosenbergii* were purchased from a farm in Chachoengsao Province, Thailand and reared per FAO guidelines. All animals used in the study were governed by regulations of IACUC of Mahidol University and approved as Animal Ethic No. MUSC61-026-428. Proteins from the gills, heart, hemocytes, ganglion, hepatopancreas, stomach and muscle tissues were extracted using tissue lysis buffer (20 mM Tris-HCl, 150 mM NaCl, 2 mM EDTA, 100 mM sodium orthovanadate, 0.5% Triton-X 100, 1x protease-inhibitor cocktail, pH 7.4). Approximately 100 μg/mL of each tissue protein lysate were diluted in coating buffer (0.1 M Na_2CO_3, 0.1 M $NaHCO_3$, pH 9.5), and coated on 96-well microtiter plates overnight at 4°C. The coated proteins were incubated with MrNV-VLPs for overnight at 4°C, followed by anti-hexahistidine tag antibody (1:1,000) and the wells were then incubated with goat anti-mouse-HRP (1:2500) For visualization, each well was incubated with a SureBlue TMB peroxidase substrate (KPL, Gaithersburg, MA). The intensity of the developed enzymatic products was detected with a spectrophotometer at 452 nm wavelength. Statistical analyses were performed using Graphpad Prism software (San Diego, CA, USA). Statistical significance between treatment groups was determined by one-way ANOVA with Dunnett's Multiple Comparison Test.

Binding of MrNV-VLPs to gill tissue lysates and tissue sections

The VLPs were incubated with either gill tissue lysate-coated 96-well Maxisorp plates (Nunc, Roskilde, Denmark) or cryo-sectioned gill tissue sections. Gill tissue lysates were prepared by homogenizing freshly extracted gill tissues from blue-claw male *M. rosenbergii*

prawn in tissue lysis. Gill tissue sections were prepared from freshly dissected gills submersed in cryoprotective solution (Tris-buffered saline and 30% glucose w/v), and snap-frozen in liquid nitrogen. The OCT blocks sectioned on a cryo-stat machine, and placed on aminopropylsilane-coated slides, then subjected to immunohistochemistry. The gill tissue lysate-coated wells or slides were incubated with MrNV-VLPs at a concentration of 20 µg/mL (equivalent to ~16 million particles) for at least 6 hr at RT detected using anti-hexahistidine tag antibodies. In order to observe the effect of lectins or monosaccharides in preventing MrNV-VLP-tissue glycan interactions, the gill tissue lysates or tissue sections were ~~either~~ pre-incubated with biotin-conjugated lectins at a concentration of 4 µg/mL, followed by incubation with MrNV-VLPs.

For chemical and enzymatic processing, gill tissue lysate-coated wells or tissue sections were treated with 20 mM sodium metaperiodate in PBS, pH 7.4 for a maximum duration of 2 hours. Enzymatic digestion with PNGase F, α1-2,3,6 mannosidase, or α1-2,3,4,6 fucosidase were conducted using the volumes and enzyme concentrations suggested by the manufacturer (New England Biolabs, MA, USA).

Binding of MrNV-VLPs to immobilized monosaccharides and glycan-coated wells

96-well Maxisorp plates (Nunc, Roskilde, Denmark) were coated with either human serum albumin (HSA-) or polyacrylamide (PAA-) conjugated monosaccharides/glycans at a concentration of 2 µg/mL in coating buffer and incubated at 4°C overnight. After extensive washing, the immobilized monosaccharides/glycans-coated wells were then treated with MrNV-VLPs 20 µg/mL (in PBS, 0.5% BSA) at 4°C overnight to examine particle-saccharide binding. The detection of VLP binding followed the ELISA methodology described above.

Binding of MrNV-VLPs to gill tissue lysates after beta-elimination treatment

Gill tissue lysates were extracted and coated to 96-well Maxisorp plates as described above. After coating and washing off excess proteins, the wells were repeatedly washed in

distilled water to prepare for the beta-elimination reaction step. 25 µL of the beta-elimination reagent from the GlycoProfile β-Elimination Kit was then added to each experimental well and then incubated overnight at 4°C. The reaction was stopped by adding 100 µL of 0.1 M HCl to each well, followed by extensive washes by distilled water and PBS before being subjected to the ELISA methodology as described above.

Release of *N*-glycans and *O*-glycans from gill tissue lysates

Tissues including gill, hepatopancreas, stomach and muscles were collected from blue-claw *M. rosenbergii*, homogenized and then lyophilized. The lyophilized tissues were resuspended in a solution of 6 M guanidine hydrochloride and 5 mM EDTA in 0.1 M Tris/HCl, pH 8.6 and agitated at 4°C overnight. The extracted glycoproteins were reduced by addition of DTT at a final concentration of 10 mM for 1 hr at 37°C, and then alkylated by addition of IAM at a final concentration of 50 mM at 37°C for 1 hr in the dark. The alkylated proteins were desalted by using dialysis membrane (MWCO 6-8000) followed by lyophilization. The recovered proteins were sequentially digested by trypsin in 50 mM ammonium bicarbonate buffer, pH 8.6 for 5 hr before chymotrypsin digestion at 37°C overnight. After brief boiling and cooling down, the glycopeptides were subjected to PNGase F digestion at 37°C, overnight.

N-glycans were fractionated from peptides mixtures by C18 Sep-Pak cartridge in 5% acetic acid. The retained peptides were eluted by 20-40% 1-propanol with 5% acetic acid, followed by drying. The eluted peptides were subjected to reductive elimination with 1M sodium borohydride in 0.05N NaOH at 37°C for 72h. The reaction was stopped by acetic acid and sample was passed through Dowex 50W-X8. After drying, borate was distilled by cp-evaporation of 10% acetic acid in methanol several times under a stream of nitrogen gas.

MALDI-MS and MS/MS analyses

Before being subjected to MS acquisition, the glycans were aliquoted for permethylation by using a modified NaOH/DMSO method (Dell et al., 1994). For MALDI-MS

glycan profiling, the permethyl derivatives were dissolved in acetonitrile, and 0.5 µL was taken to be mixed with 0.5 µL of 2,5-dihydroxybenzoic acid (DHB) matrix (10 mg/mL in acetonitrile), spotted on the target plate. Data acquisition was performed manually on a 4800 Proteomics Analyzer (Applied Biosystems) operated in the reflectron mode. MALDI-MS/MS sequencing of the permethylated glycans was performed on MALDI-QIT-TOF (Shimadzu) with the same spotting method.

Pull-down assay and Far Western blotting

The pull-down assay using Ni-NTA-immobilized 6xHis tagged proteins as bait was modified from a previously described method (Louche, Salcedo, & Bigot, 2017). 200 µg of purified MrNV-VLPs with a 6xHis tag were added to 1 mL Ni-NTA beads (GE Healthcare, Piscataway, NJ. The MrNV-VLP-bound Ni-NTA beads were then incubated with gill proteins by passing lysates through the resin-bed. The beads with bound gill proteins were eluted with 1 mM NaCl, 250 mM imidazole-containing buffer. Gill proteins, MrNV-VLPs and MrNV-VLP-bound gill proteins were subjected to SDS-PAGE on 12.5% polyacrylamide gel, followed by Coomassie Blue G250 staining. The same set of proteins were also transferred onto PVDF membrane. Membrane 1 was incubated with MrNV-VLPs (20 µg/mL) followed by anti-6xHis-tag antibody (1:1000) and goat anti- mouse HRP (1:2500), membrane 2 was incubated with biotin conjugated AAL lectin (1:1000) followed by streptavidin-HRP (1:2500) and membrane 3 was incubated with AAL lectin for 3 hrs. at RT followed by MrNV-VLPs (20 µg/mL) which were detected using anti-6xHis-tag antibodies. The immunoreactive bands were visualized by an enhanced chemiluminescence kit (Amersham Pharmacia, Buckinghamshire, UK).

650 **FIGURE LEGENDS**

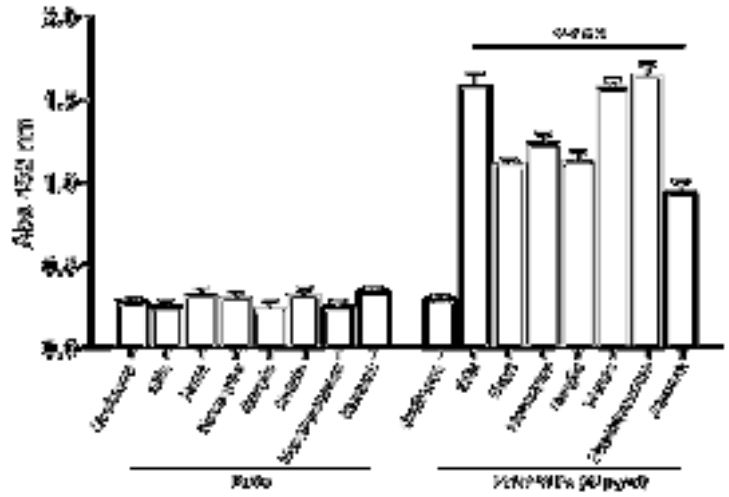

651

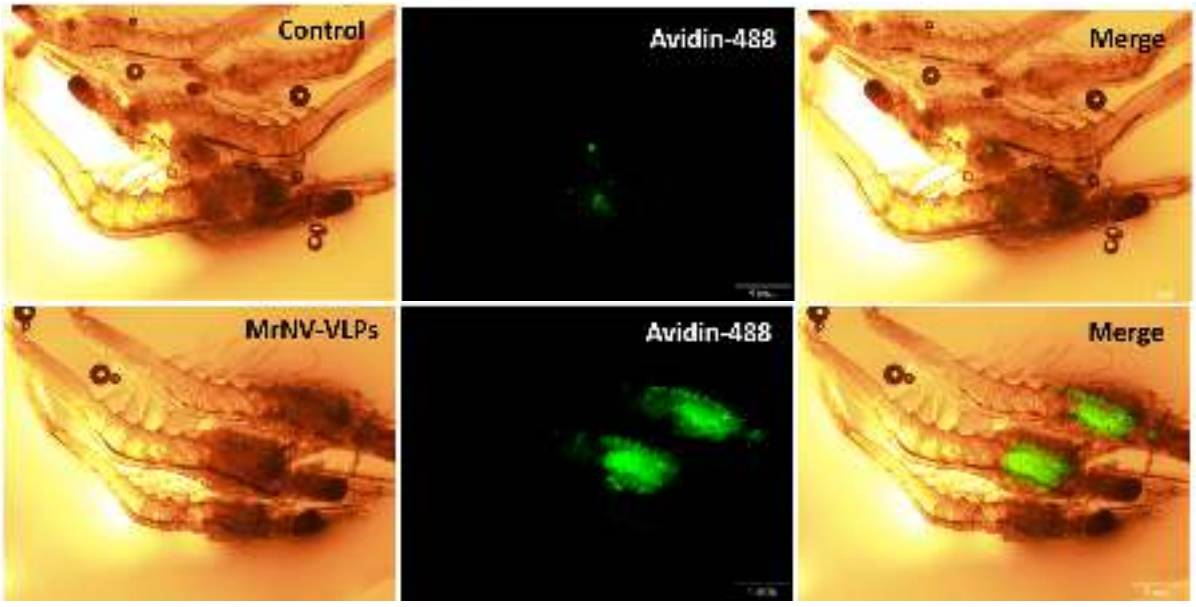

652

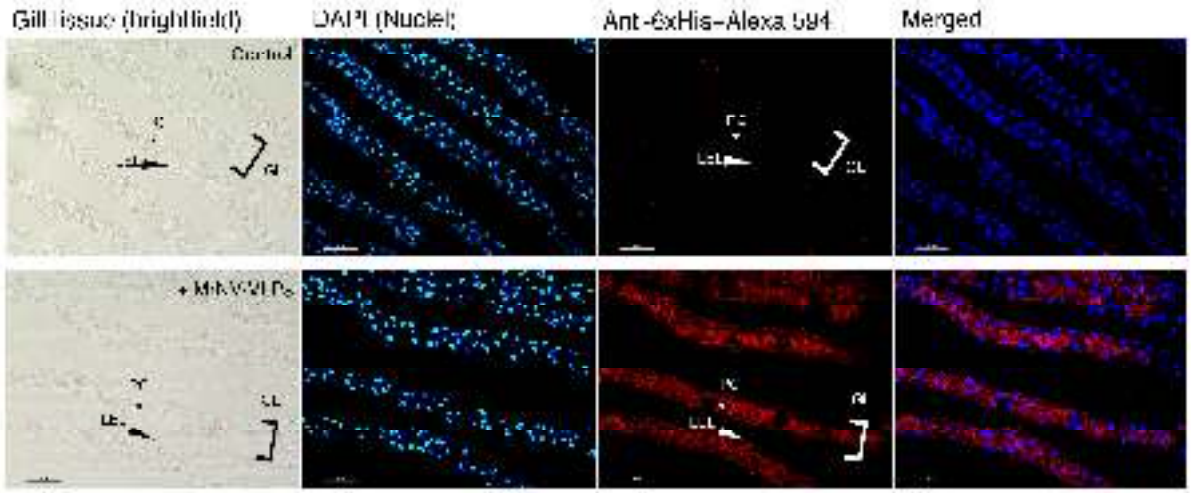

653

Figure 1. MrNV-VLPs exhibit a high preference for gill tissues. (A) ELISA showed that MrNV VLPs can generally bind to the selected tissue lysates (****p<0.0001 when compared to buffer control group). Values are the means ± SD of triplicate results. (B) MrNV-VLPs tracked by immunofluorescence (green) were highly localized to the carapace-covered gills of post-larvae whole-mount specimens. (C) In gill tissue sections, the MrNV-VLPs (red signals - Alexa 594) were localized throughout the gill lamellae (GL), especially at the pillar cells (PC) and lamellar epithelium lining (LEL) (2nd row, panels 3 and 4) when compared to the control (1st row). Bars = 50 μm.

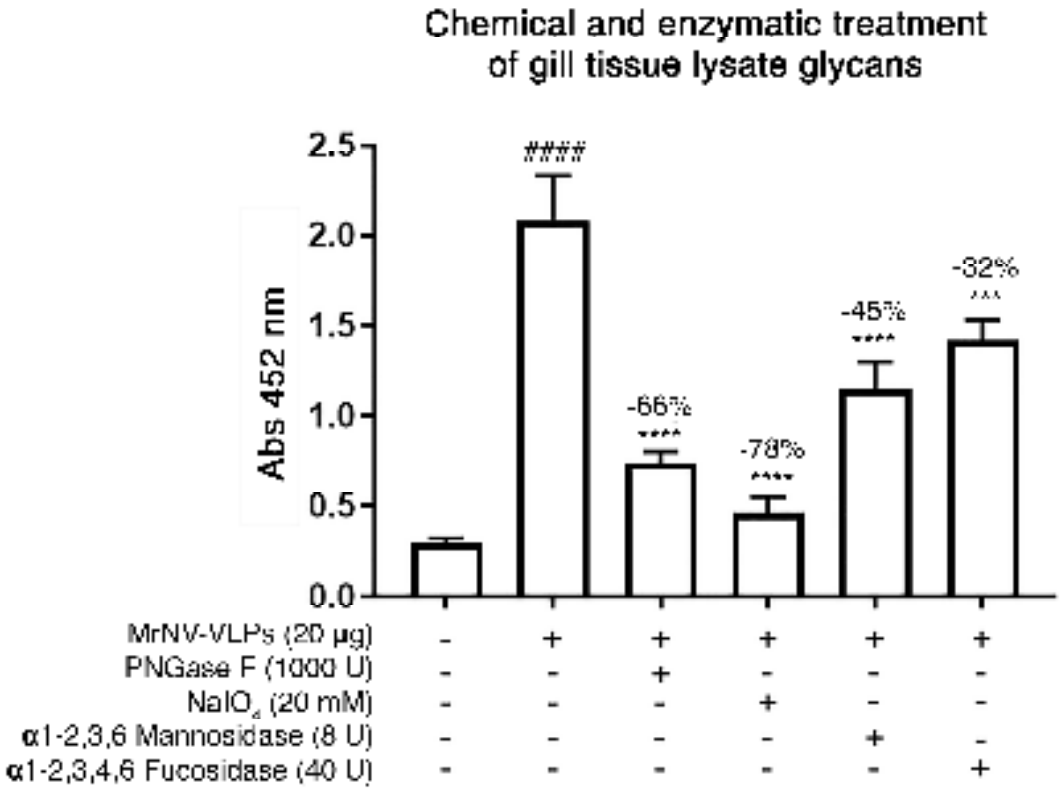

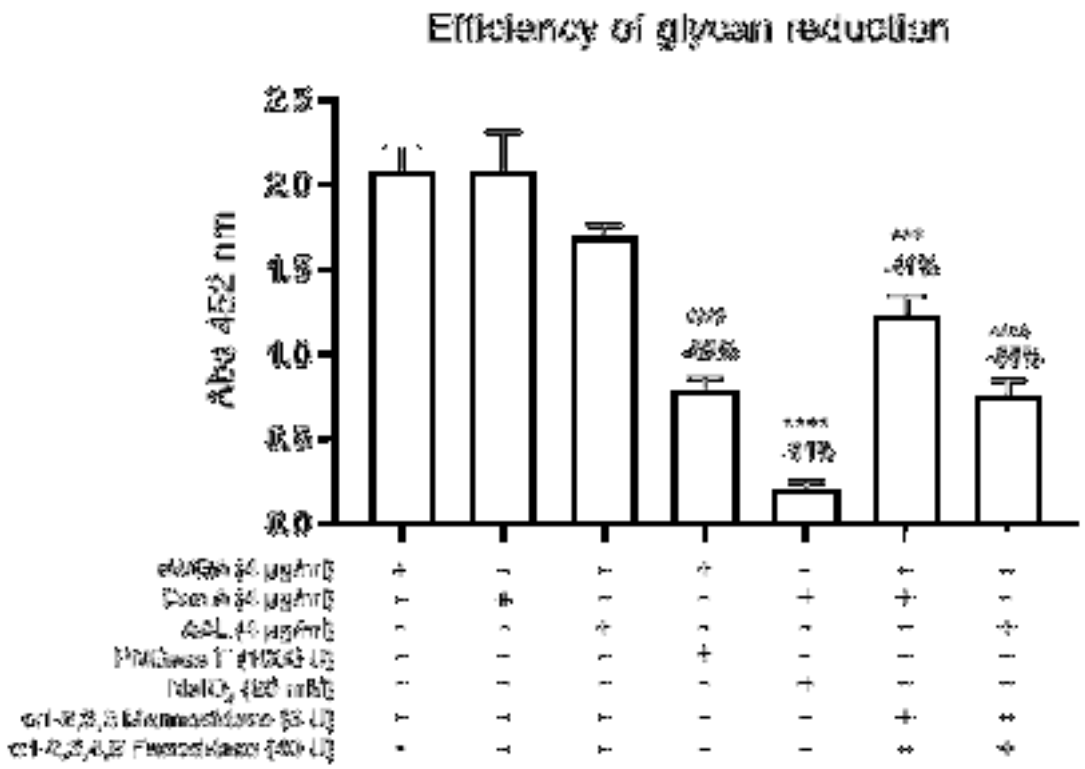
Efficiency of glycan reduction
Abs 452 nm
2.5
2.0
1.5
1.0
0.5
0.0
****
-91%
-87%

663

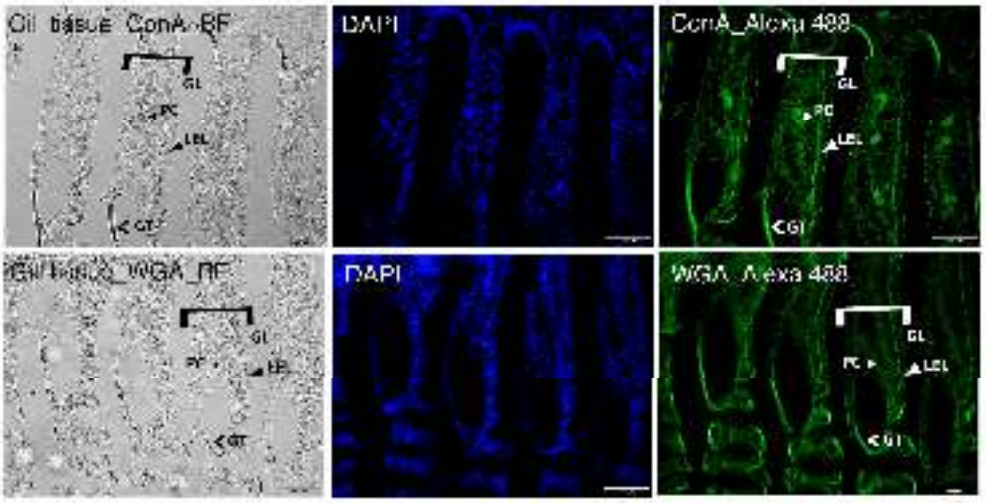
Oil tissue ConA_BF
DAPI
ConA_Alexa 488
GL
PC
LEL
CGI
WGA_BF
DAPI
WGA_Alexa 488

664

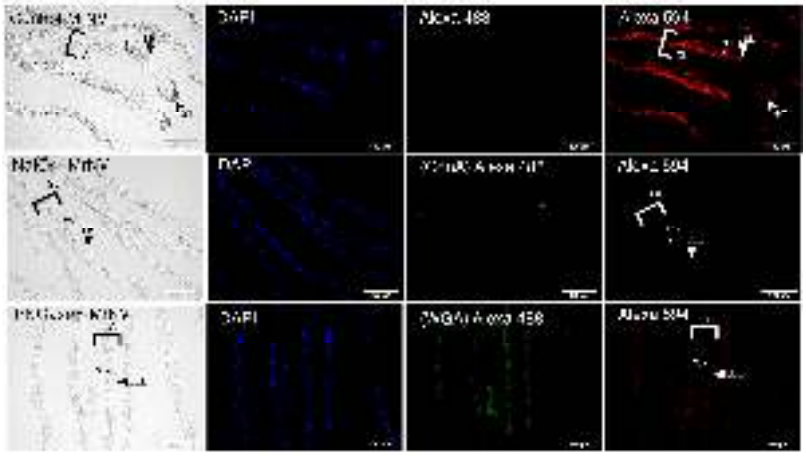

Figure 2. MrNV-VLP binding to gill tissue lysates and sections depends on glycans. (A) ELISA experiments showed treatment of lysates with sodium metaperiodate resulted in the highest level of reduction of MrNV-VLP binding ($^{\#\#\#\#}p<0.0001$ when compared to buffer control group; *p < 0.05, **p < 0.01, ***p < 0.001, ****p<0.0001 when compared to the MrNV-VLP-only treated group) Values are the means ± SD of triplicate results from two independent experiments. The graph in (B) shows the efficiency of glycan reduction of each of the substances or enzymes used using lectins binding as indicators. ($^{\#\#\#\#}p<0.0001$ when compared to the sWGA-treated group; ***p < 0.001 and ****p<0.0001 when compared to the Con A-treated group; ^^^^p<0.0001 when compared to the AAL-treated group) Values are the means ± SD of triplicate results from two independent experiments. (C) demonstrates the extensive binding of Con A and sWGA lectins (green) throughout the gill lamellae GL, including the lamellar epithelial lining (LEL), pillar cells (PC) and gill tips (GT). (D) sodium metaperiodate treatment virtually abolished MrNV-VLP binding (red) to the gill tissues (row 2, column 4) when compared to normal MrNV-VLP binding patterns (row 1, column 4). PNGase F was capable of reducing some level of binding (row 3, column 4). The lectins Con A (row 2, column 3) and sWGA (row 3, column 3) verified sodium metaperiodate and PNGase F reduced glycan levels. GL = gill lamellae, LEL = lamellar epithelial lining, PC = pillar cells, GL = gill tips. Bars = 100 μm.

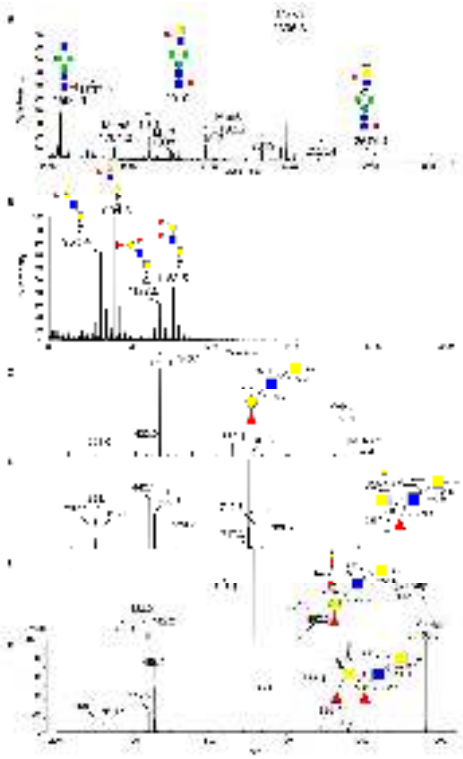

Figure 3. Mass spectrometry analyses of gill tissues reveal the presence of unique fucosylated glycans. MALDI-MS profiles of permethylated *N*-glycans (A) and *O*-glycans (B) isolated from the gill tissue lysates are shown, respectively. All signals were annotated and assigned according to MS/MS analyses. The peaks labeled with * in (A) are polyHexose signals. Symbols used here: square, HexNAc; circle, Hex; triangle, Fuc. -itol reduced form. MS/MS spectra of the ions at *m/z* 953, 994, 1127 and 1168 corresponding to $Fuc_1Hex_1HexNAc_1$-HexNAc-itol (C), $Fuc_1HexNAc_2$-HexNAc-itol (D), $Fuc_2Hex_1HexNAc_1$-HexNAc-itol (E), and $Fuc_2HexNAc_2$-HexNAc-itol (F), respectively, were shown and schematically illustrated. The peaks labeled with # in MS/MS spectra (C, D, E) are fragment ions with a further loss of 74 mass units from fragment Z ions, and these ions were assigned as elimination of carbon 2, 3-substitutes of HexNAc. Glycosidic oxygen atoms are drawn out to discriminate between cleavages at either side of the oxygen.

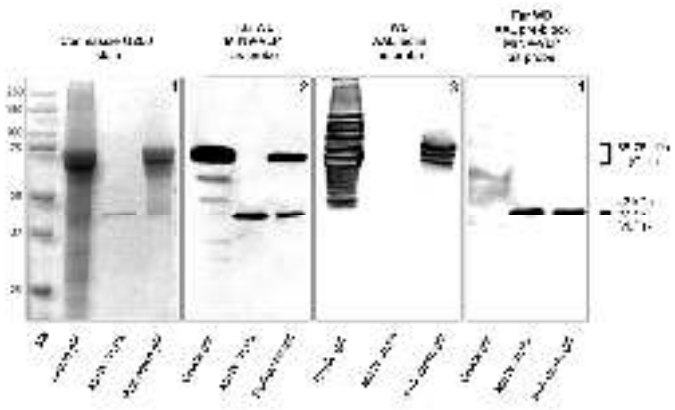

Figure 4. Far Western blotting of gill proteins with MrNV-VLPs and blocking by AAL pre-incubation. Crude gill proteins, MrNV-VLPs, and gill proteins obtained from pull-down assay were run alongside each other on the same SDS-PAGE gel and then subjected to Coomassie staining (panel 1), transferred and followed by Far Western blot using MrNV-VLP as the bait (panel 2), Western blot with AAL lectin as a probe (panel 3), and AAL pre-blocking followed by Far Western blot using MrNV-VLPs as the bait (panel 4). The MrNV-VLP lane (42 kDa band) served as a positive control for anti-6xHis antibodies used in the Far Western blots. The gill proteins from the pull-down assay showed major bands at 65-75 kDa.

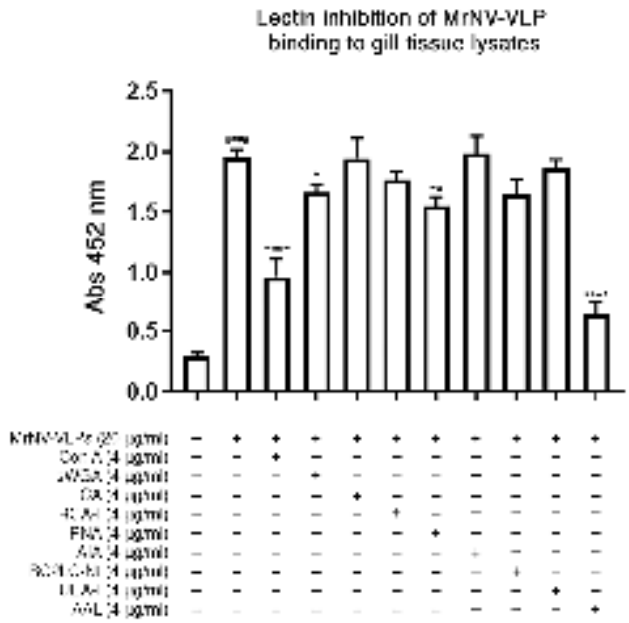

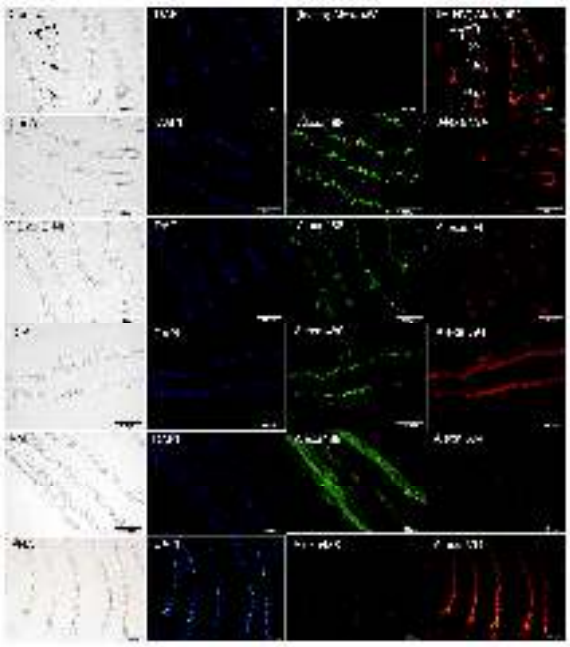

Figure 5. Lectin inhibition of MrNV-VLP binding to gill tissue lysates and sections. (A) ELISA experiments of MrNV-VLPs binding to gill tissue lysate coated wells preincubated with different lectins showed AAL to cause the highest level of inhibition of particle binding ($^{\#\#\#\#}$p<0.0001 when compared to buffer control group; *p < 0.05, **p < 0.01, ***p < 0.001, ****p<0.0001 when compared to MrNV-VLP-only treated group). (B) Immunofluorescence staining of gill tissues by pre-incubation with biotinylated lectins (green), followed by incubation with MrNV-VLP (red). As shown in the panel (row 4, column 4), AAL was able to almost completely abolish the signals of MrNV-VLP binding to the gill tissues. GL = gill lamellae, LEL = lamellar epithelial lining, PC = pillar cells, GL = gill tips. Bars = 100 μm.

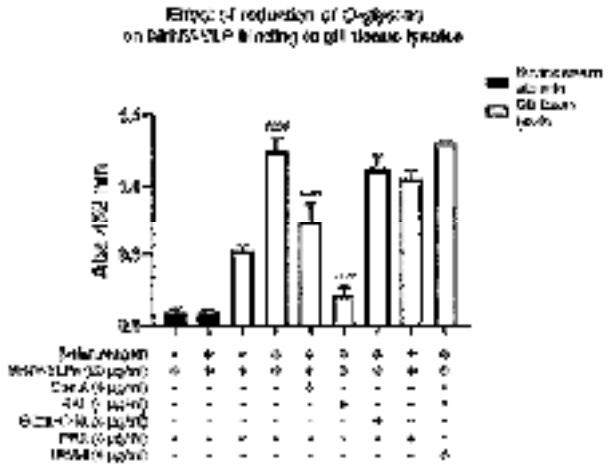

Figure 6. Beta-elimination treatment of gill tissue lysates reveals the low dependence on *O*-glycans for MrNV-VLP binding. Gill tissue lysates pre-treatment with beta-elimination reagent resulted in a significant increase in VLP binding levels, indicating either low dependence on *O*-glycans, or more access to *N*-glycans. Post-treating the reagent pre-treated lysates with Con A and AAL, resulted in highly significant reduction in VLP binding levels compared to the BC2L-C-Nt, PNA and UEA-I; suggesting a preference for *N*-glycans over *O*-glycans ($^{\#\#\#\#}p < 0.0001$ when compared to beta-elimination reagent-treated lysates; ****$p < 0.0001$ when compared to reagent-treated lysates incubated with MrNV-VLPs). Values are the means ± SD of triplicate results.

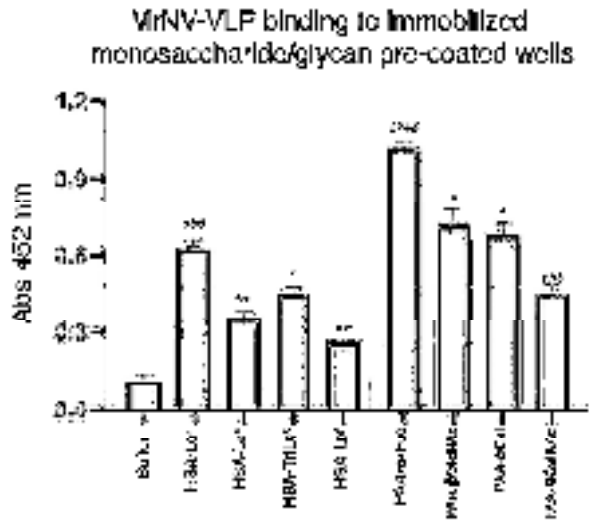

729

730 **Figure 7. MrNV-VLPs exhibit binding to immobilized fucosylated glycoconjugates-**
731 **coated wells.** MrNV-VLPs showed the highest level of binding towards 96-well ELISA plates
732 pre-coated with polyacrylamide-conjugated alpha-fucose (PAA-α-Fucose), followed by PAA-
733 GlcNAc, PAA-Gal, and PAA-GalNAc ($^{\#\#\#\#}p<0.0001$ when compared to buffer control group;
734 $^p < 0.01$, $^{\wedge\wedge}p < 0.01$ and $^{\wedge\wedge\wedge}p<0.001$ when compared to PAA-α-Fuc). MrNV-VLPs showed
735 binding to the more complex fucosylated Lewis antigens, with the highest level of binding to
736 HSA-Lewis a ($^{\#\#\#}p<0.0001$ when compared to buffer control group; $^*p < 0.01$ and $^{**}p < 0.01$
737 when compared to HSA-Le^a). Values are the means ± SD of triplicate results.

738

739

740 **ACKNOWLEDGMENTS**

741 This work was supported by Thailand Research Fund (TRF: Grant No. MRG6180055);
742 Faculty of Science, Mahidol University, University Research Grant (493/2559) of
743 Srinakharinwirot University, Ministère des Affaires Etrangères et Européennes (Programme
744 Régional Bio-Asie) and from INSERM UMR 1232, Nantes, France. The authors would also
745 like to thank the Franco-Thai Junior Fellowship Program 2019 and all the scientists at the

Center of Nanoimaging (CNI) and the Central Instrument Facility at the Faculty of Science, Mahidol University and at the Faculty of Medicine, Srinakharinwirot University.

DECLARATION OF CONFLICTING INTERESTS

The authors declare no conflicting interests in preparing this article.

REFERENCES

Almand, E. A., Moore, M. D., & Jaykus, L. A. (2017). Norovirus Binding to Ligands Beyond Histo-Blood Group Antigens. *Front Microbiol, 8*, 2549. doi:10.3389/fmicb.2017.02549

Ashok, A., & Atwood, W. J. (2006). Virus receptors and tropism. *Adv Exp Med Biol, 577*, 60-72. doi:10.1007/0-387-32957-9_4

771 Azad, I. S., Shekhar, M. S., Thirunavukkarasu, A. R., Poornima, M., Kailasam, M., Rajan, J.
772 J., . . . Ravichandran, P. (2005). Nodavirus infection causes mortalities in hatchery
773 produced larvae of Lates calcarifer: first report from India. *Dis Aquat Organ, 63*(2-3),
774 113-118. doi:10.3354/dao063113
775 Baldus, S. E., Thiele, J., Park, Y.-O., Hanisch, F.-G., Bara, J., & Fischer, R. (1996).
776 Characterization of the binding specificity ofAnguilla anguilla agglutinin (AAA) in
777 comparison toUlex europaeus agglutinin I (UEA-I). *Glycoconjugate journal, 13*(4),
778 585-590.
779 Bergstrom, M., Astrom, E., Pahlsson, P., & Ohlson, S. (2012). Elucidating the selectivity of
780 recombinant forms of Aleuria aurantia lectin using weak affinity chromatography. *J*
781 *Chromatogr B Analyt Technol Biomed Life Sci, 885-886*, 66-72.
782 doi:10.1016/j.jchromb.2011.12.015
783 Bonami, J.-R., Shi, Z., Qian, D., & Sri Widada, J. (2005). White tail disease of the giant
784 freshwater prawn, Macrobrachium rosenbergii: separation of the associated virions
785 and characterization of MrNV as a new type of nodavirus. *Journal of Fish Diseases,*
786 *28*(1), 23-31. doi:10.1111/j.1365-2761.2004.00595.x
787 Bonami, J.-R., & Widada, J. S. (2011). Viral diseases of the giant fresh water prawn
788 Macrobrachium rosenbergii: a review. *Journal of invertebrate pathology, 106*(1), 131-
789 142.
790 Bonami, J. R., Shi, Z., Qian, D., & Sri Widada, J. (2005). White tail disease of the giant
791 freshwater prawn, Macrobrachium rosenbergii: separation of the associated virions
792 and characterization of MrNV as a new type of nodavirus. *J Fish Dis, 28*(1), 23-31.
793 doi:10.1111/j.1365-2761.2004.00595.x
794 Chang, J. S., & Chi, S. C. (2015). GHSC70 is involved in the cellular entry of nervous
795 necrosis virus. *J Virol, 89*(1), 61-70. doi:10.1128/JVI.02523-14

796 Dell, A., Reason, A. J., Khoo, K. H., Panico, M., McDowell, R. A., & Morris, H. R. (1994).
797 Mass spectrometry of carbohydrate-containing biopolymers. *Methods Enzymol, 230*,
798 108-132. doi:10.1016/0076-6879(94)30010-0
799 Felgenhauer, B. E. (1992). Internal anatomy of the Decapoda: an overview.
800 Freire, C. A., Onken, H., & McNamara, J. C. (2008). A structure-function analysis of ion
801 transport in crustacean gills and excretory organs. *Comp Biochem Physiol A Mol*
802 *Integr Physiol, 151*(3), 272-304. doi:10.1016/j.cbpa.2007.05.008
803 Gagneux, P., & Varki, A. (1999). Evolutionary considerations in relating oligosaccharide
804 diversity to biological function. *Glycobiology, 9*(8), 747-755.
805 Gangnonngiw, W., Bunnontae, M., Phiwsaiya, K., Senapin, S., & Dhar, A. K. (2020). In
806 experimental challenge with infectious clones of Macrobrachium rosenbergii
807 nodavirus (MrNV) and extra small virus (XSV), MrNV alone can cause mortality in
808 freshwater prawn (Macrobrachium rosenbergii). *Virology, 540*, 30-37.
809 doi:10.1016/j.virol.2019.11.004
810 Garenaux, E., Maes, E., Leveque, S., Brassart, C., & Guerardel, Y. (2011). Structural
811 characterization of complex O-linked glycans from insect-derived material.
812 *Carbohydr Res, 346*(9), 1093-1104. doi:10.1016/j.carres.2011.04.008
813 Gaunitz, S., Jin, C., Nilsson, A., Liu, J., Karlsson, N. G., & Holgersson, J. (2013). Mucin-
814 type proteins produced in the Trichoplusia ni and Spodoptera frugiperda insect cell
815 lines carry novel O-glycans with phosphocholine and sulfate substitutions.
816 *Glycobiology, 23*(7), 778-796. doi:10.1093/glycob/cwt015
817 Hameed, A. S., Yoganandhan, K., Widada, J. S., & Bonami, J. (2004). Experimental
818 transmission and tissue tropism of Macrobrachium rosenbergii nodavirus (MrNV) and
819 its associated extra small virus (XSV). *Diseases of Aquatic Organisms, 62*(3), 191-
820 196.

821 Hayakijkosol, O., & Owens, L. (2013). Non-permissive C6/36 cell culture for the Australian
822 isolate of Macrobrachium rosenbergii nodavirus. *J Fish Dis, 36*(4), 401-409.
823 doi:10.1111/j.1365-2761.2012.01414.x
824 Henry, R. P., Lucu, C., Onken, H., & Weihrauch, D. (2012). Multiple functions of the
825 crustacean gill: osmotic/ionic regulation, acid-base balance, ammonia excretion, and
826 bioaccumulation of toxic metals. *Front Physiol, 3*, 431.
827 doi:10.3389/fphys.2012.00431
828 Ho, K. L., Gabrielsen, M., Beh, P. L., Kueh, C. L., Thong, Q. X., Streetley, J., . . . Bhella, D.
829 (2018). Structure of the Macrobrachium rosenbergii nodavirus: A new genus within
830 the Nodaviridae? *PLoS Biol, 16*(10), e3000038. doi:10.1371/journal.pbio.3000038
831 Ho, K. L., Kueh, C. L., Beh, P. L., Tan, W. S., & Bhella, D. (2017). Cryo-Electron
832 Microscopy Structure of the Macrobrachium rosenbergii Nodavirus Capsid at 7
833 Angstroms Resolution. *Sci Rep, 7*(1), 2083. doi:10.1038/s41598-017-02292-0
834 Hsieh, C.-Y., Wu, Z.-B., Tung, M.-C., Tu, C., Lo, S.-P., Chang, T.-C., . . . Tsai, S.-S. (2006).
835 In situ hybridization and RT-PCR detection of Macrobrachium rosenbergii nodavirus
836 in giant freshwater prawn, Macrobrachium rosenbergii (de Man), in Taiwan. *Journal*
837 *of Fish Diseases, 29*(11), 665-671. doi:10.1111/j.1365-2761.2006.00762.x
838 Hsu, T. A., Takahashi, N., Tsukamoto, Y., Kato, K., Shimada, I., Masuda, K., . . .
839 Betenbaugh, M. J. (1997). Differential N-glycan patterns of secreted and intracellular
840 IgG produced in Trichoplusia ni cells. *J Biol Chem, 272*(14), 9062-9070.
841 doi:10.1074/jbc.272.14.9062
842 Huang, L.-Y., Halder, S., & Agbandje-McKenna, M. (2014). Parvovirus glycan interactions.
843 *Current opinion in virology, 7*, 108-118.
844 Hykollari, A., Malzl, D., Stanton, R., Eckmair, B., & Paschinger, K. (2019). Tissue-specific
845 glycosylation in the honeybee: Analysis of the N-glycomes of Apis mellifera larvae

and venom. *Biochim Biophys Acta Gen Subj, 1863*(11), 129409. doi:10.1016/j.bbagen.2019.08.002

Jariyapong, P., Chotwiwatthanakun, C., Somrit, M., Jitrapakdee, S., Xing, L., Cheng, H. R., & Weerachatyanukul, W. (2014). Encapsulation and delivery of plasmid DNA by virus-like nanoparticles engineered from Macrobrachium rosenbergii nodavirus. *Virus Res, 179*, 140-146. doi:10.1016/j.virusres.2013.10.021

Jayasankar, V., Tsutsui, N., Jasmani, S., Saido-Sakanaka, H., Yang, W. J., Okuno, A., . . . Wilder, M. N. (2002). Dynamics of vitellogenin mRNA expression and changes in hemolymph vitellogenin levels during ovarian maturation in the giant freshwater prawn Macrobrachium rosenbergii. *Journal of Experimental Zoology, 293*(7), 675-682.

Jean-Michel, A., François, H., Donald, V. L., Rita, M. R., Jocelyne, M., & Jean-Robert, B. (1999). A viral disease associated with mortalities in hatchery-reared postlarvae of the giant freshwater prawn Macrobrachium rosenbergii. *Diseases of Aquatic Organisms, 38*(3), 177-181.

Kubelka, V., Altmann, F., Staudacher, E., Tretter, V., Marz, L., Hard, K., . . . Vliegenthart, J. F. (1993). Primary structures of the N-linked carbohydrate chains from honeybee venom phospholipase A2. *Eur J Biochem, 213*(3), 1193-1204. doi:10.1111/j.1432-1033.1993.tb17870.x

Kurz, S., Aoki, K., Jin, C., Karlsson, N. G., Tiemeyer, M., Wilson, I. B., & Paschinger, K. (2015). Targeted release and fractionation reveal glucuronylated and sulphated N- and O-glycans in larvae of dipteran insects. *J Proteomics, 126*, 172-188. doi:10.1016/j.jprot.2015.05.030

Kurz, S., King, J. G., Dinglasan, R. R., Paschinger, K., & Wilson, I. B. (2016). The fucomic potential of mosquitoes: Fucosylated N-glycan epitopes and their cognate

fucosyltransferases. *Insect Biochem Mol Biol, 68*, 52-63. doi:10.1016/j.ibmb.2015.11.001

Le Pendu, J. (2004). Histo-blood group antigen and human milk oligosaccharides: genetic polymorphism and risk of infectious diseases. *Adv Exp Med Biol, 554*, 135-143. doi:10.1007/978-1-4757-4242-8_13

Le Pendu, J., & Ruvoën-Clouet, N. (2019). Fondness for sugars of enteric viruses confronts them with human glycans genetic diversity. *Human genetics*, 1-8.

Leonard, R., Rendic, D., Rabouille, C., Wilson, I. B., Preat, T., & Altmann, F. (2006). The Drosophila fused lobes gene encodes an N-acetylglucosaminidase involved in N-glycan processing. *J Biol Chem, 281*(8), 4867-4875. doi:10.1074/jbc.M511023200

Liu, W., Hsu, C. H., Hong, Y. R., Wu, S. C., Wang, C. H., Wu, Y. M., . . . Lin, C. S. (2005). Early endocytosis pathways in SSN-1 cells infected by dragon grouper nervous necrosis virus. *J Gen Virol, 86*(Pt 9), 2553-2561. doi:10.1099/vir.0.81021-0

Louche, A., Salcedo, S., & Bigot, S. (2017). Protein–Protein Interactions: Pull-Down Assays. In (Vol. 1615, pp. 247-255).

Low, C. F., Syarul Nataqain, B., Chee, H. Y., Rozaini, M. Z. H., & Najiah, M. (2017). Betanodavirus: Dissection of the viral life cycle. *J Fish Dis, 40*(11), 1489-1496. doi:10.1111/jfd.12638

Martini, F., Eckmair, B., Stefanic, S., Jin, C., Garg, M., Yan, S., . . . Paschinger, K. (2019). Highly modified and immunoactive N-glycans of the canine heartworm. *Nat Commun, 10*(1), 75. doi:10.1038/s41467-018-07948-7

Matsumura, K., Higashida, K., Ishida, H., Hata, Y., Yamamoto, K., Shigeta, M., . . . Taniguchi, N. (2007). Carbohydrate binding specificity of a fucose-specific lectin from Aspergillus oryzae: a novel probe for core fucose. *J Biol Chem, 282*(21), 15700-15708. doi:10.1074/jbc.M701195200

McGaw, I. J. (2005). The decapod crustacean circulatory system: a case that is neither open nor closed. *Microsc Microanal, 11*(1), 18-36. doi:10.1017/S1431927605050026

NaveenKumar, S., Shekar, M., Karunasagar, I., & Karunasagar, I. (2013). Genetic analysis of RNA1 and RNA2 of Macrobrachium rosenbergii nodavirus (MrNV) isolated from India. *Virus Res, 173*(2), 377-385. doi:10.1016/j.virusres.2013.01.003

North, S. J., Koles, K., Hembd, C., Morris, H. R., Dell, A., Panin, V. M., & Haslam, S. M. (2006). Glycomic studies of Drosophila melanogaster embryos. *Glycoconj J, 23*(5-6), 345-354. doi:10.1007/s10719-006-6693-4

Okuno, A., Yang, W. J., Jayasankar, V., Saido-Sakanaka, H., Huong, D. T. T., Jasmani, S., . . . Ohira, T. (2002). Deduced primary structure of vitellogenin in the giant freshwater prawn, Macrobrachium rosenbergii, and yolk processing during ovarian maturation. *Journal of Experimental Zoology, 292*(5), 417-429.

Paschinger, K., & Wilson, I. B. (2015). Two types of galactosylated fucose motifs are present on N-glycans of Haemonchus contortus. *Glycobiology, 25*(6), 585-590. doi:10.1093/glycob/cwv015

Paschinger, K., & Wilson, I. B. H. (2019). Comparisons of N-glycans across invertebrate phyla. *Parasitology, 146*(14), 1733-1742. doi:10.1017/S0031182019000398

Prasanphanich, N. S., Luyai, A. E., Song, X., Heimburg-Molinaro, J., Mandalasi, M., Mickum, M., . . . Cummings, R. D. (2014). Immunization with recombinantly expressed glycan antigens from Schistosoma mansoni induces glycan-specific antibodies against the parasite. *Glycobiology, 24*(7), 619-637. doi:10.1093/glycob/cwu027

Prasanphanich, N. S., Mickum, M. L., Heimburg-Molinaro, J., & Cummings, R. D. (2013). Glycoconjugates in host-helminth interactions. *Front Immunol, 4*, 240. doi:10.3389/fimmu.2013.00240

921 Raman, R., Tharakaraman, K., Sasisekharan, V., & Sasisekharan, R. (2016). Glycan-protein
922 interactions in viral pathogenesis. *Curr Opin Struct Biol, 40*, 153-162.
923 doi:10.1016/j.sbi.2016.10.003
924 Rendić, D., Wilson, I. B., & Paschinger, K. (2008). The glycosylation capacity of insect cells.
925 *Croatica Chemica Acta, 81*(1), 7-21.
926 Sahul Hameed, A. S., Yoganandhan, K., Sri Widada, J., & Bonami, J. R. (2004).
927 Experimental transmission and tissue tropism of Macrobrachium rosenbergii
928 nodavirus (MrNV) and its associated extra small virus (XSV). *Dis Aquat Organ,*
929 *62*(3), 191-196. doi:10.3354/dao062191
930 Schachter, H. (2009). Paucimannose N-glycans in Caenorhabditis elegans and Drosophila
931 melanogaster. *Carbohydr Res, 344*(12), 1391-1396. doi:10.1016/j.carres.2009.04.028
932 Shanker, S., Hu, L., Ramani, S., Atmar, R. L., Estes, M. K., & Venkataram Prasad, B. V.
933 (2017). Structural features of glycan recognition among viral pathogens. *Curr Opin*
934 *Struct Biol, 44*, 211-218. doi:10.1016/j.sbi.2017.05.007
935 Smit, C. H., van Diepen, A., Nguyen, D. L., Wuhrer, M., Hoffmann, K. F., Deelder, A. M., &
936 Hokke, C. H. (2015). Glycomic Analysis of Life Stages of the Human Parasite
937 Schistosoma mansoni Reveals Developmental Expression Profiles of Functional and
938 Antigenic Glycan Motifs. *Mol Cell Proteomics, 14*(7), 1750-1769.
939 doi:10.1074/mcp.M115.048280
940 Somrit, M., Watthammawut, A., Chotwiwatthanakun, C., Ounjai, P., Suntimanawong, W., &
941 Weerachatyanukul, W. (2017). C-terminal domain on the outer surface of the
942 Macrobrachium rosenbergii nodavirus capsid is required for Sf9 cell binding and
943 internalization. *Virus research, 227*, 41-48.
944 Somrit, M., Watthammawut, A., Chotwiwatthanakun, C., & Weerachatyanukul, W. (2016).
945 The key molecular events during Macrobrachium rosenbergii nodavirus (MrNV)

946 infection and replication in Sf9 insect cells. *Virus research, 223*, 1-9.
947 doi:10.1016/j.virusres.2016.06.012
948 Sri Widada, J., Durand, S., Cambournac, I., Qian, D., Shi, Z., Dejonghe, E., . . . Bonami, J. R.
949 (2003). Genome-based detection methods of Macrobrachium rosenbergii nodavirus, a
950 pathogen of the giant freshwater prawn, Macrobrachium rosenbergii: dot-blot, in situ
951 hybridization and RT-PCR. *Journal of Fish Diseases, 26*(10), 583-590.
952 doi:10.1046/j.1365-2761.2003.00493.x
953 Stanton, R., Hykollari, A., Eckmair, B., Malzl, D., Dragosits, M., Palmberger, D., . . .
954 Paschinger, K. (2017). The underestimated N-glycomes of lepidopteran species.
955 *Biochim Biophys Acta Gen Subj, 1861*(4), 699-714. doi:10.1016/j.bbagen.2017.01.009
956 Staudacher, E. (2015). Mucin-Type O-Glycosylation in Invertebrates. *Molecules, 20*(6),
957 10622-10640. doi:10.3390/molecules200610622
958 Stencel-Baerenwald, J. E., Reiss, K., Reiter, D. M., Stehle, T., & Dermody, T. S. (2014). The
959 sweet spot: defining virus-sialic acid interactions. *Nature Reviews Microbiology,*
960 *12*(11), 739-749. doi:10.1038/nrmicro3346
961 Stroh, L. J., & Stehle, T. (2014). Glycan Engagement by Viruses: Receptor Switches and
962 Specificity. *Annu Rev Virol, 1*(1), 285-306. doi:10.1146/annurev-virology-031413-
963 085417
964 Sudhakaran, R., Haribabu, P., Kumar, S. R., Sarathi, M., Ahmed, V. P., Babu, V. S., . . .
965 Hameedl, A. S. (2008). Natural aquatic insect carriers of Macrobrachium rosenbergii
966 nodavirus (MrNV) and extra small virus (XSV). *Dis Aquat Organ, 79*(2), 141-145.
967 doi:10.3354/dao01886
968 Sudhakaran, R., Parameswaran, V., & Sahul Hameed, A. S. (2007). In vitro replication of
969 Macrobrachium rosenbergii nodavirus and extra small virus in C6/36 mosquito cell
970 line. *J Virol Methods, 146*(1-2), 112-118. doi:10.1016/j.jviromet.2007.06.011

971 Sulak, O., Cioci, G., Lameignere, E., Balloy, V., Round, A., Gutsche, I., . . . Imberty, A.
972 (2011). Burkholderia cenocepacia BC2L-C is a super lectin with dual specificity and
973 proinflammatory activity. *PLoS Pathog, 7*(9), e1002238.
974 doi:10.1371/journal.ppat.1002238
975 Thompson, A. J., de Vries, R. P., & Paulson, J. C. (2019). Virus recognition of glycan
976 receptors. *Curr Opin Virol, 34*, 117-129. doi:10.1016/j.coviro.2019.01.004
977 Tiemeyer, M., Nakato, H., & Esko, J. D. (2015). Arthropoda. In rd, A. Varki, R. D.
978 Cummings, J. D. Esko, P. Stanley, G. W. Hart, M. Aebi, A. G. Darvill, T. Kinoshita,
979 N. H. Packer, J. H. Prestegard, R. L. Schnaar, & P. H. Seeberger (Eds.), *Essentials of*
980 *Glycobiology* (pp. 335-349). Cold Spring Harbor (NY): Cold Spring Harbor
981 Laboratory Press

984 van Die, I., & Cummings, R. D. (2010). Glycan gimmickry by parasitic helminths: a strategy
985 for modulating the host immune response? *Glycobiology, 20*(1), 2-12.
986 doi:10.1093/glycob/cwp140
987 Varki, A. (2006). Nothing in glycobiology makes sense, except in the light of evolution. *Cell,*
988 *126*(5), 841-845. doi:10.1016/j.cell.2006.08.022
989 Varki, A. (2017). Biological roles of glycans. *Glycobiology, 27*(1), 3-49.
990 doi:10.1093/glycob/cww086
991 Walski, T., De Schutter, K., Van Damme, E. J. M., & Smagghe, G. (2017). Diversity and
992 functions of protein glycosylation in insects. *Insect Biochem Mol Biol, 83*, 21-34.
993 doi:10.1016/j.ibmb.2017.02.005
994 Wimmerova, M., Mitchell, E., Sanchez, J. F., Gautier, C., & Imberty, A. (2003). Crystal
995 structure of fungal lectin: six-bladed beta-propeller fold and novel fucose recognition

mode for Aleuria aurantia lectin. *J Biol Chem, 278*(29), 27059-27067. doi:10.1074/jbc.M302642200

Yan, S., Wilson, I. B., & Paschinger, K. (2015). Comparison of RP-HPLC modes to analyse the N-glycome of the free-living nematode Pristionchus pacificus. *Electrophoresis, 36*(11-12), 1314-1329. doi:10.1002/elps.201400528

Zhang, L., & Ten Hagen, K. G. (2019). O-Linked glycosylation in Drosophila melanogaster. *Curr Opin Struct Biol, 56*, 139-145. doi:10.1016/j.sbi.2019.01.014

Zhu, F., Li, D., & Chen, K. (2019). Structures and functions of invertebrate glycosylation. *Open Biol, 9*(1), 180232. doi:10.1098/rsob.180232

SUPPLEMENTARY FIGURES

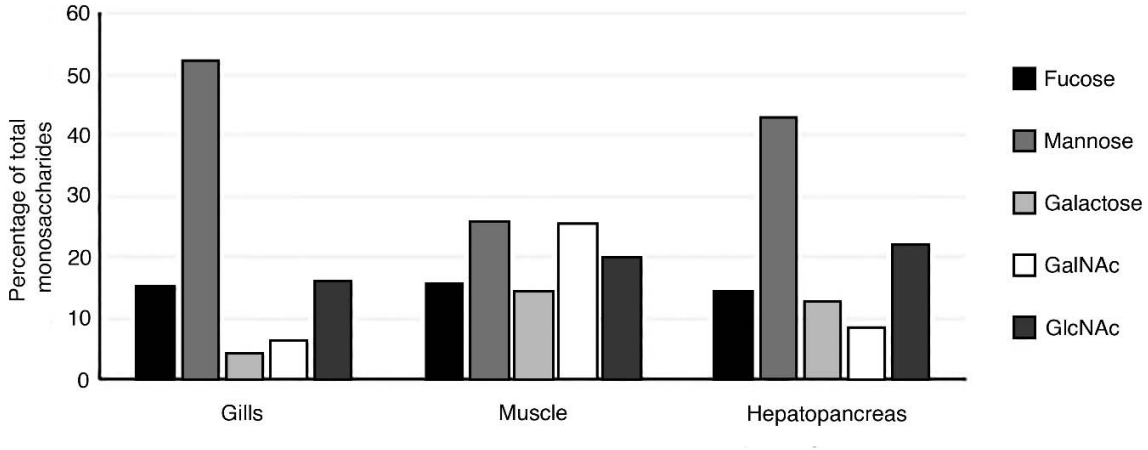

Supplementary figure 1. Proportion of monosaccharides in hepatopancreas, muscle, and gill tissues as revealed by GC-MS. The chart shows the proportions of the main monosaccharides fucose (Fuc), mannose (Man), galactose (Gal), *N*-acetylgalactosamine (GalNAc) and *N*-acetylglucosamine (GlcNAc) from total monosaccharides extracted from the three tissues.

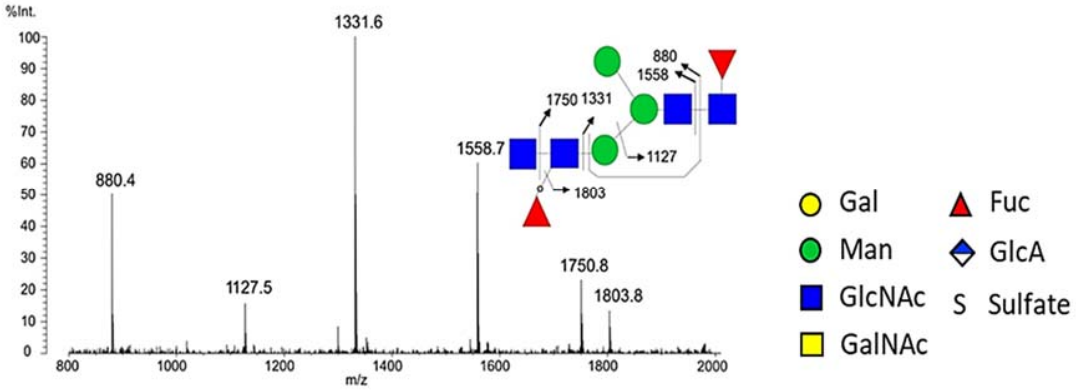

Supplementary figure 2. MS/MS spectrum of permethylated *N*-glycans from gill tissue.

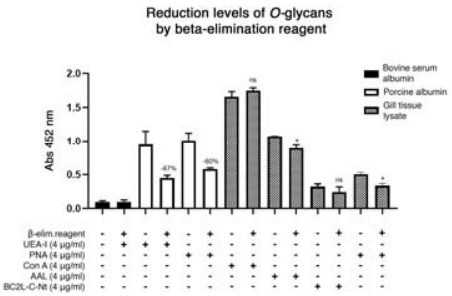

Supplementary figure 3. Efficiency of the removal of O-glycans using beta-elimination reagents. The reduction of O-glycans by the process was first confirmed by examining the level of binding by O-glycan-binding lectins such as UEA-I and PNA to porcine mucins treated by the beta-elimination reagent. There was at least a 60% reduction in O-glycans in the mucin-coated wells (white bars). There was a possible slight reduction in O-glycan levels after treatment with the reagent as shown by the levels of AAL, BC2L-C-Nt and PNA binding (gray bars, *p<0.05). Non-significant (ns) reduction in Con A binding, indicated *N*-glycans were unaffected by the reagent. Values are the means ± SD of triplicate results.

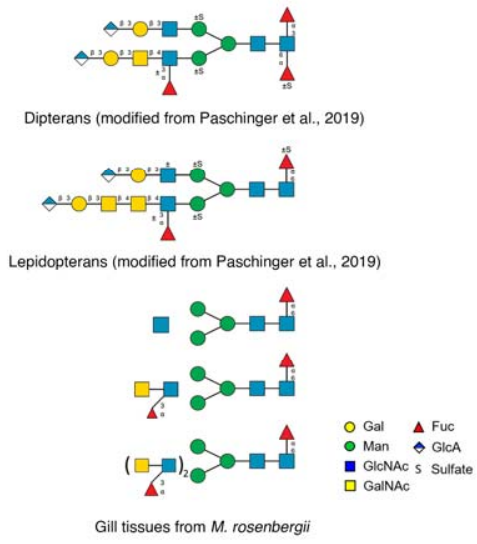

Supplementary figure 4. Comparison of *N*-glycans between dipteran, lepidopteran and in the gills of *M. rosenbergii.*

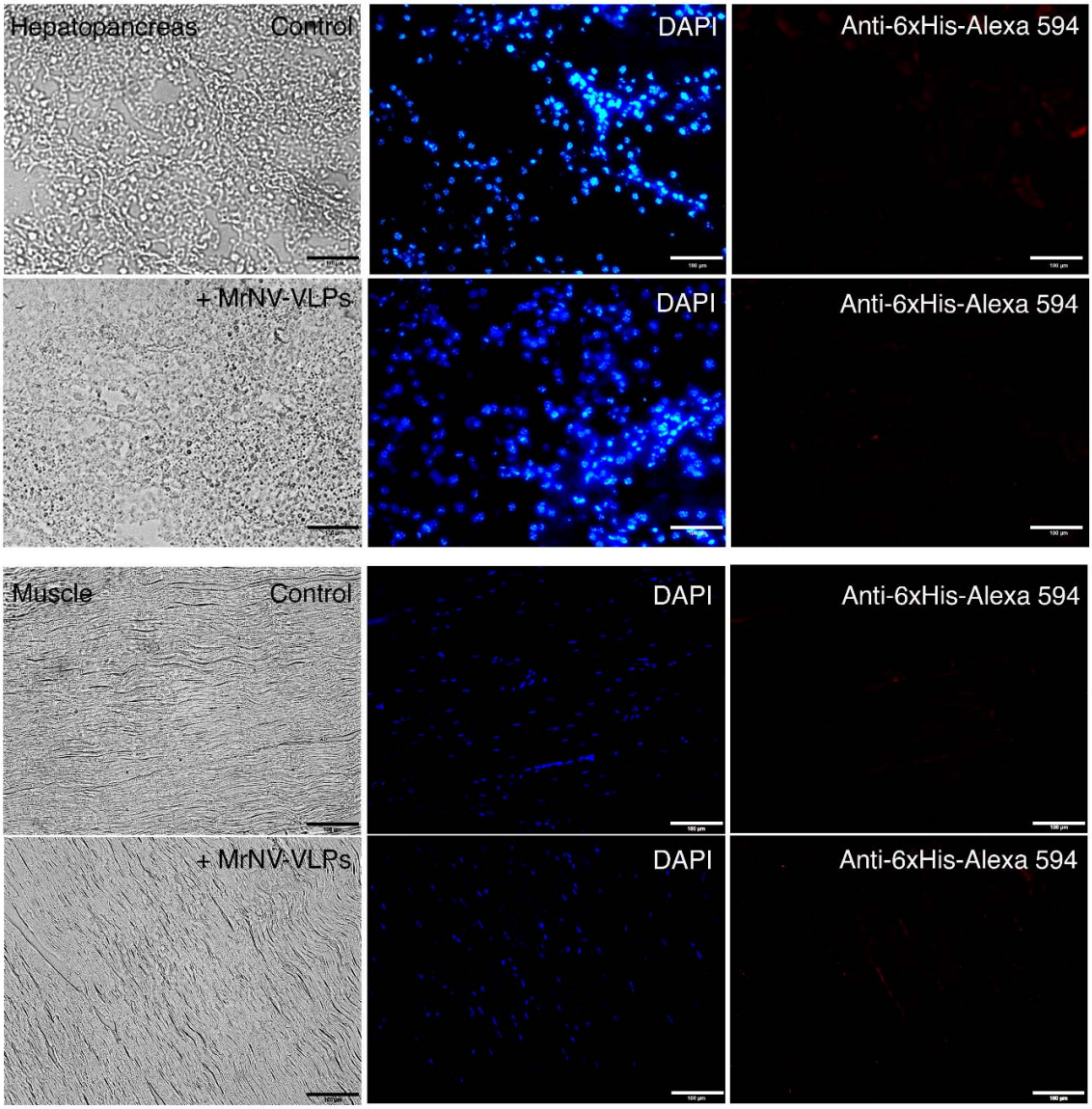

Supplementary figure 5. Low binding levels of MrNV-VLPs to hepatopancreas and muscle tissues in *M. rosenbergii.* MrNV-VLPs (red signals – Alexa 594, 3rd column) did not exhibit notable levels of binding to hepatopancreas and muscles tissues (rows 2 and 4) when compared to gill tissues shown in Figure 1C. Bars = 100 μm.

SUPPLEMENTARY FIGURE LEGENDS

Supplementary figure 1. Proportion of monosaccharides in hepatopancreas, muscle, and gill tissues as revealed by GC-MS. The chart shows the proportions of the main monosaccharides fucose (Fuc), mannose (Man), galactose (Gal), *N*-acetylgalactosamine (GalNAc) and *N*-acetylglucosamine (GlcNAc) from total monosaccharides extracted from the three tissues.

Supplementary figure 2. MS/MS spectrum of permethylated *N*-glycans from gill tissue.

Supplementary figure 3. Efficiency of the removal of O-glycans using beta-elimination reagents. The reduction of O-glycans by the process was first confirmed by examining the level of binding by O-glycan-binding lectins such as UEA-I and PNA to porcine mucins treated by the beta-elimination reagent. There was at least a 60% reduction in O-glycans in the mucin-coated wells (white bars). There was a possible slight reduction in O-glycan levels after treatment with the reagent as shown by the levels of AAL, BC2L-C-Nt and PNA binding (gray bars, *$p<0.05$). Non-significant (ns) reduction in Con A binding, indicated *N*-glycans were unaffected by the reagent. Values are the means ± SD of triplicate results.

Supplementary figure 4. Comparison of *N*-glycans between dipteran, lepidopteran and in the gills of *M. rosenbergii.*

Supplementary figure 5. Low binding levels of MrNV-VLPs to hepatopancreas and muscle tissues in *M. rosenbergii.* MrNV-VLPs (red signals – Alexa 594, 3rd column) did not exhibit

notable levels of binding to hepatopancreas and muscles tissues (rows 2 and 4) when compared to gill tissues shown in Figure 1C. Bars = 100 μm.